ELSEVIER
SAUNDERS

Neurosurg Clin N Am 19 (2008) 175–205

NEUROSURGERY
CLINICS
OF NORTH AMERICA

Imaging of Acoustic Neuromas

Hugh D. Curtin, MD[a,*], William L. Hirsch, Jr, MD[b]

[a]*Massachusetts Eye and Ear Infirmary, Harvard Medical School, Boston, MA, USA*
[b]*Radiologic Physicians Associates, Fairmont, WV, USA*

Imaging has become a sensitive method of evaluating patients with possible acoustic neuromas (ANs). Magnetic resonance imaging (MRI) continues to evolve but is already considered the preferred imaging study for the evaluation of a patient with suspected AN [1–13]. A negative gadolinium-enhanced MRI examination is considered a reliable indicator that the patient does not have an AN. Other imaging techniques remain as useful tools in certain clinical settings, but many techniques, considered state of the art less than a decade ago, have faded into almost complete obsolescence [3].

Imaging of the eighth cranial nerve sheath tumors has progressed from plain radiography to today's MRI [14]. In this evolution, the evaluation has progressed from attempts to show subtle findings that suggested the possibility of a lesion to actual visualization of the smallest of tumors deep within the internal auditory canal (IAC) itself. Because of the increasing acceptance of MRI as the imaging procedure of choice, much of the following discussion deals with MRI. Other modalities, such as computed tomography (CT), are discussed where appropriate. Imaging strategies in various clinical situations are discussed.

It should be remembered that either gadolinium-enhanced MRI or contrast-enhanced CT can demonstrate almost any AN [2]. The usual clinical situation, however, is that the clinician is trying to ensure that the patient does not have an AN, and so the most desirable test is the one that is the most sensitive. CT may not visualize the intracanalicular region well, and it is here that MRI establishes its advantage.

Anatomy and imaging

The bony anatomy is demonstrated in excellent detail by high-resolution CT when performed with a bone algorithm. The cortical edges of the IAC are sharply defined, and intricate internal anatomy of the labyrinth is routinely visualized. The bone algorithm allows limited visualization of the soft tissues, however, and the contents of the IAC are not seen.

The soft tissue or standard algorithm gives an improved visualization of the soft tissues, but the contrast of the nerves versus the cerebrospinal fluid (CSF) is still insufficient to allow demonstration of the fine soft tissue elements within the IAC. In addition, there is still a problem of artifact streaking obscuring the region of the porus acusticus and the cerebello-pontine angle (CPA) cistern.

MRI, on the other hand, gives excellent soft tissue visualization but does not show the bony detail nearly as well as CT. Cortical bone gives a lack of signal or signal void on MRI. Air also is seen as a lack of signal on the MRI scan. In a normal situation, therefore, the observer is not able to differentiate the otic capsule from the air-filled middle ear. Both appear black. The petrous apex often contains fat, which is seen as bright signal on the T_1-weighted (short TR/TE) image.

Fluid does give some signal on the T_1-weighted image. Fluid is not nearly as bright as fat but still can be seen quite easily, especially when contrasted against the signal void of the dense bone of the inner ear. Thus the perilymph/endolymph in the labyrinth and the CSF in the IAC can be seen on the image (see Fig. 1A).

The article of originally appeared in Otolaryngologic Clinics of NA: Volume 25, issue 3, June 1992; p. 553–608.

* Corresponding author. Hugh D. Curtin, MD, 230 Lothrop Street, Pittsburgh, PA 15213.

1042-3680/08/$ - see front matter
doi:10.1016/j.nec.2008.02.012

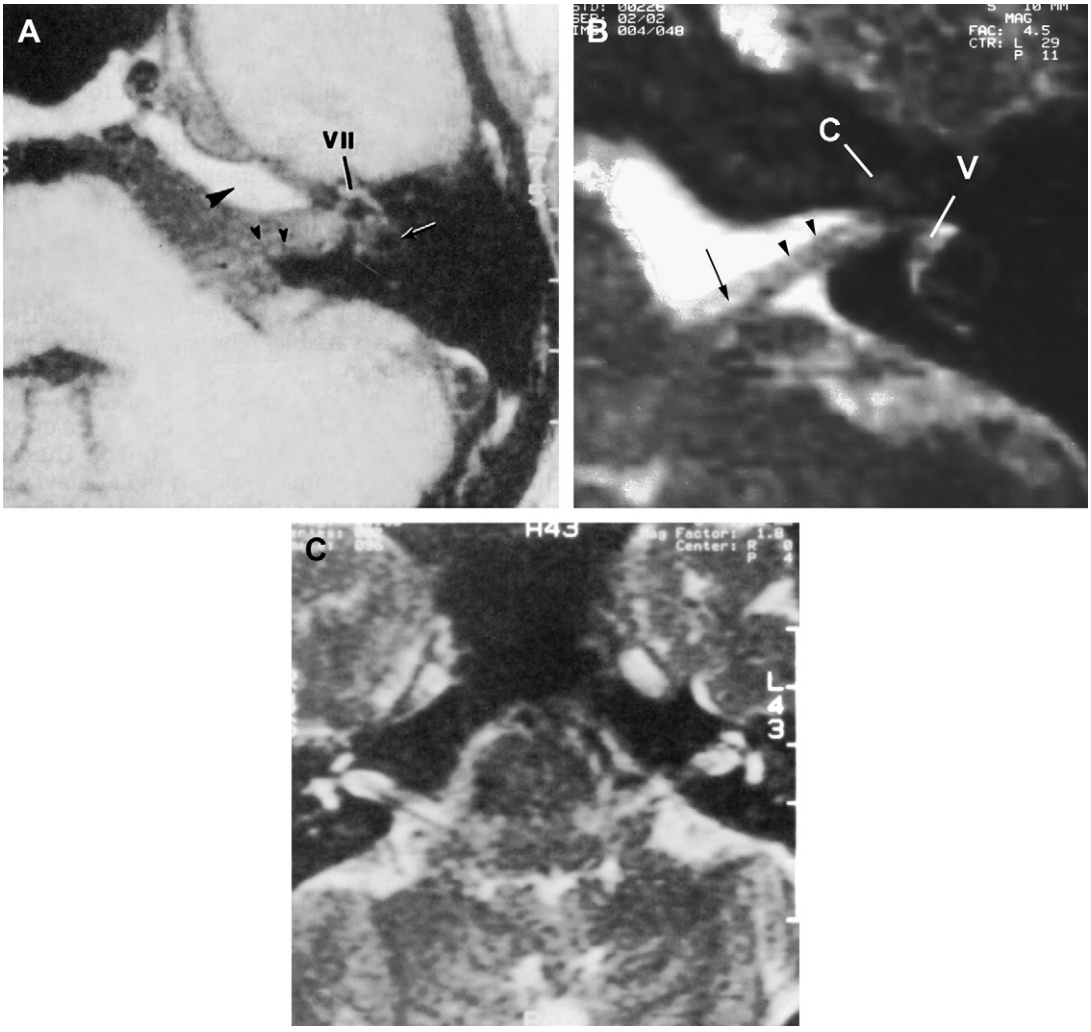

Fig. 1. (*A*) T_1-weighted (TR 600/TE 20) magnetic resonance image of the temporal bones. There is enough signal from the soft tissue of the facial nerve (VII) and the fluid in the internal auditory canal (IAC) as well as in the horizontal semicircular canal (*arrow*) to allow visualization contrasted against the mastoid and otic capsule. Note that the fluid and soft tissue signal is not nearly as bright as the fat (*large arrowhead*) in the petrous apex. *Small arrowheads* indicate neural elements. (*B*) T_2-weighted image (TR 2500/TE 90) turns the cerebrospinal fluid and the fluid in the vestibule (V) bright white. The intermediate signal from the cochlea (C) does not indicate that there is tissue within but rather that there is partial volume effect. The bright fluid in the cochlea is averaged with the contiguous bone to give an intermediate signal intensity. Nerve elements in the IAC (*arrowheads*) are extending from the root exit zone at the pontomedullary junction (*arrow*). (*C*) Extreme T_2-weighted image (TR 4000/TE 120) shows the bright signal in the cochlea, the vestibules, and IAC. On the right side a nerve can be seen from the pontomedullary junction to the fundus of the IAC.

On the T_1-weighted image, the soft tissue and the CSF have different signal intensities. Soft tissues such as the nerves (or brain) have somewhat greater signal than the CSF. Often the nerves can be seen crossing the CPA cistern and occasionally can be followed into the IAC (see Fig. 1A) [28,48]. The differences in signal intensity are not great enough on a T_1-weighted image to see the actual nerves consistently within the canal and to follow the nerves to their exit points at the lateral aspect of the canal [15].

The T_2-weighted (long TR/TE) image can be used to increase the signal difference between the nerves and the surrounding fluid (Fig. 1B, C). A

heavily T_2-weighted image makes fluid bright relative to the soft tissues. Thus the nerves can be seen more frequently if thin enough slices are obtained. The relative signal intensity from the labyrinth also increases, and so the inner ear structure may also be more conspicuous.

Acoustic neuroma

The appearance of an AN depends on the internal architecture of the tumor, its site of origin along the neural pathway, and the size of the lesion as well as the specifics of the imaging procedure being performed. The tumor can have a somewhat variable internal architecture. The tumor is made up of various concentrations of Antoni A and Antoni B type histologic patterns. Both types can often be identified within the same tumor. This variability of histology along with the presence of cystic areas and even small hemorrhages is thought to account for the wide spectrum of appearance of the AN.

An AN is a soft tissue tumor. Although the lesion can certainly come into contact with the brain, the role of imaging is usually to try to contrast the lesion against the CSF. It may be difficult to appreciate an AN on CT done without contrast administration because the density differences are insufficient for consistent visualization. On MRI without contrast administration, the tumor has a different appearance than CSF (Figs. 2 and 3). The tumor is brighter than CSF on a T_1-weighted image. The appearance on a T_2-weighted image is variable. The small intracanalicular tumors have, in our experience, been consistently darker than CSF on heavily T_2-weighted images (Fig. 4).

On MRI without contrast enhancement, small or even fairly large cystic areas can often be appreciated within the tumor. These cysts may be dark or bright on a T_1-weighted image. Bright signal may represent small areas of hemorrhage, [16]. but an elevated protein content within a cyst could result in a similar phenomenon (Fig. 5).

Virtually all ANs have an altered blood–brain barrier [17]. Thus on either MRI or CT, the tumors enhance after intravenous injection of a contrast agent that crosses such an abnormal blood–brain barrier. This phenomenon is responsible for the now classic appearance of the AN on both CT and MR [4,18] (Figs. 6–9).

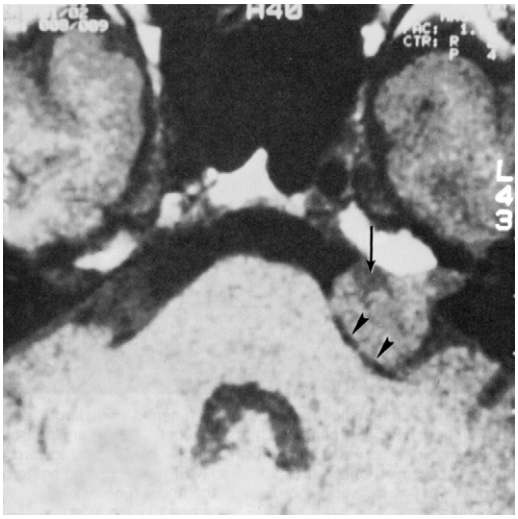

Fig. 2. T_1-weighted magnetic resonance image without contrast, acoustic neuroma left side. The tumor flattens against the cerebellar peduncle (*arrowheads*). A small area of lower signal intensity represents a cystic area (*arrow*). The lesion can be followed into the internal auditory canal.

The tumor shows as a bright white lesion protruding from the IAC on CT (see Figs. 6A and 7). On the MR image, the bright white of the high signal from the enhancing tumor is seen on the T_1-weighted image (see Figs. 8 and 9). There have been scattered reports of nonenhancing ANs, but if they exist, they are exceedingly rare. Some authors have recommended that, at least with CT, the contrast agent be injected 10 to 15 minutes before imaging to allow the contrast agent time to cross the blood–brain barrier into the lesion [19]. This has not seemed to be a problem on MRI.

Frequently the entire tumor enhances uniformly. If there are cystic regions within the lesion, they may not enhance, and the fluid contained within the cystic areas will have the same appearance after contrast administration as before (Fig. 10). These are avascular collections, so the contrast agent cannot reach the material within the cavity.

Calcifications are occasionally mentioned as rarely being present in ANs. They are extremely uncommon. In fact, if anything more than minimal calcification is present, an alternative diagnosis, such as meningioma, should be considered. Calcifications, when present, are expected to be tiny, and they are unlikely to be seen on

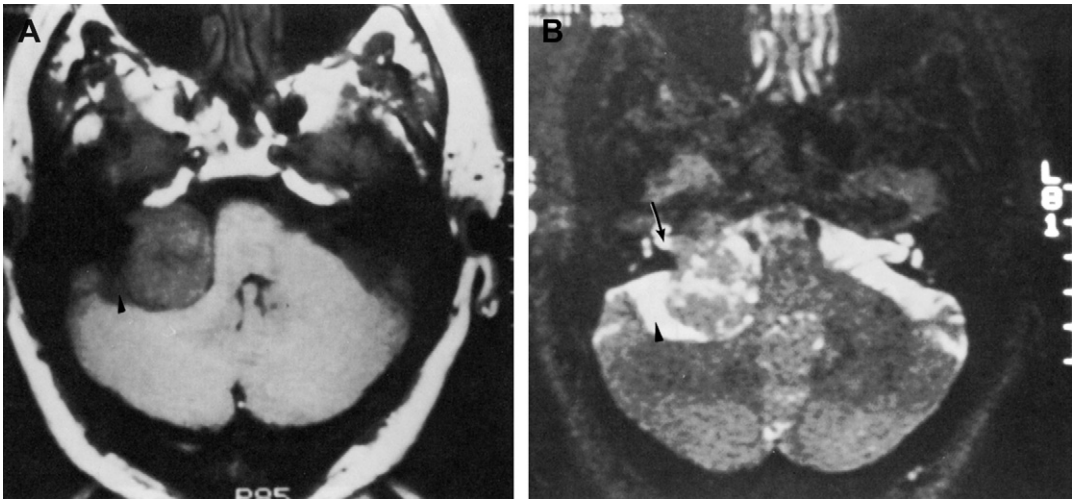

Fig. 3. (*A*) T_1-weighted magnetic resonance image (unenhanced); large acoustic neuroma is seen filling the internal auditory canal (IAC) and cerebellopontine angle cistern. The pons and the cerebellar peduncle as well as the fourth ventricle are pushed toward the contralateral side. There is a collection of cerebrospinal fluid (CSF) (*arrowhead*) posterolateral to the acoustic neuroma. (*B*) T_2-weighted image shows the acoustic neuroma in the cistern protruding into the IAC. A small amount of CSF is trapped in the lateral aspect of the IAC (*arrow*), thus the tumor is not completely filling the canal. The fluid collection posterolateral to the neuroma (*arrowhead*) shows the same brightening as the CSF.

MRI, where small calcifications are averaged together with contiguous soft tissue and become virtually invisible. CT is much more likely to show small flecks of calcium if they are present.

The shape of an AN is determined by its point of origin and its size. These lesions are thought to arise at or near the glial–Schwann cell junction. This junction point is usually found just inside the IAC, but the actual site is variable enough that

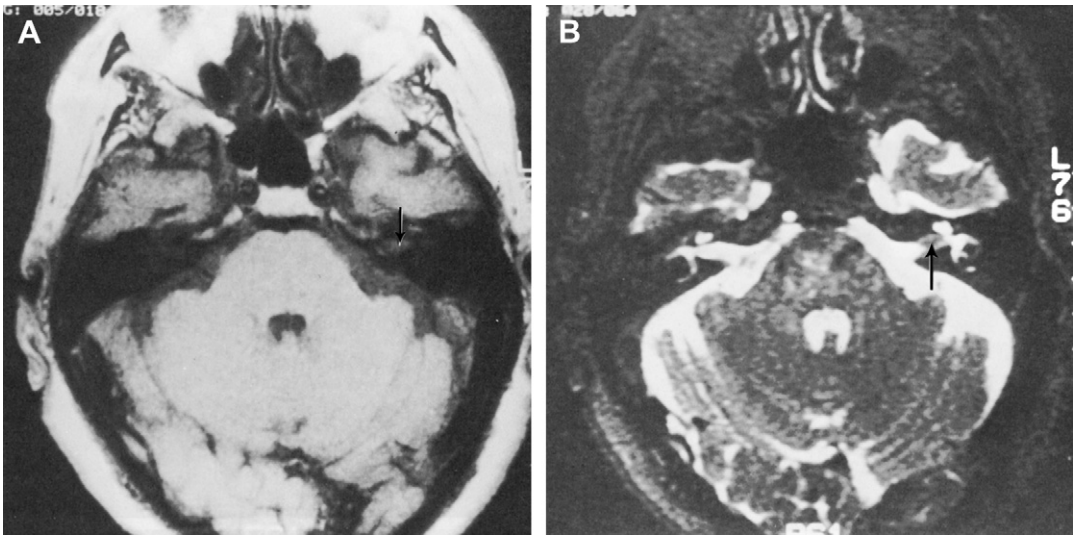

Fig. 4. (*A*) T_1-weighted magnetic resonance image (without gadolinium). There is a slight increase in signal on the side of the acoustic neuroma (*arrow*). This would be difficult to call positive with certainty. (*B*) On a T_2-weighted image the cerebrospinal fluid (CSF) is bright white. The tumor now shows as an area of low signal (*arrow*) contrasted against the CSF. Compare with the CSF-filled internal auditory canal on the normal side.

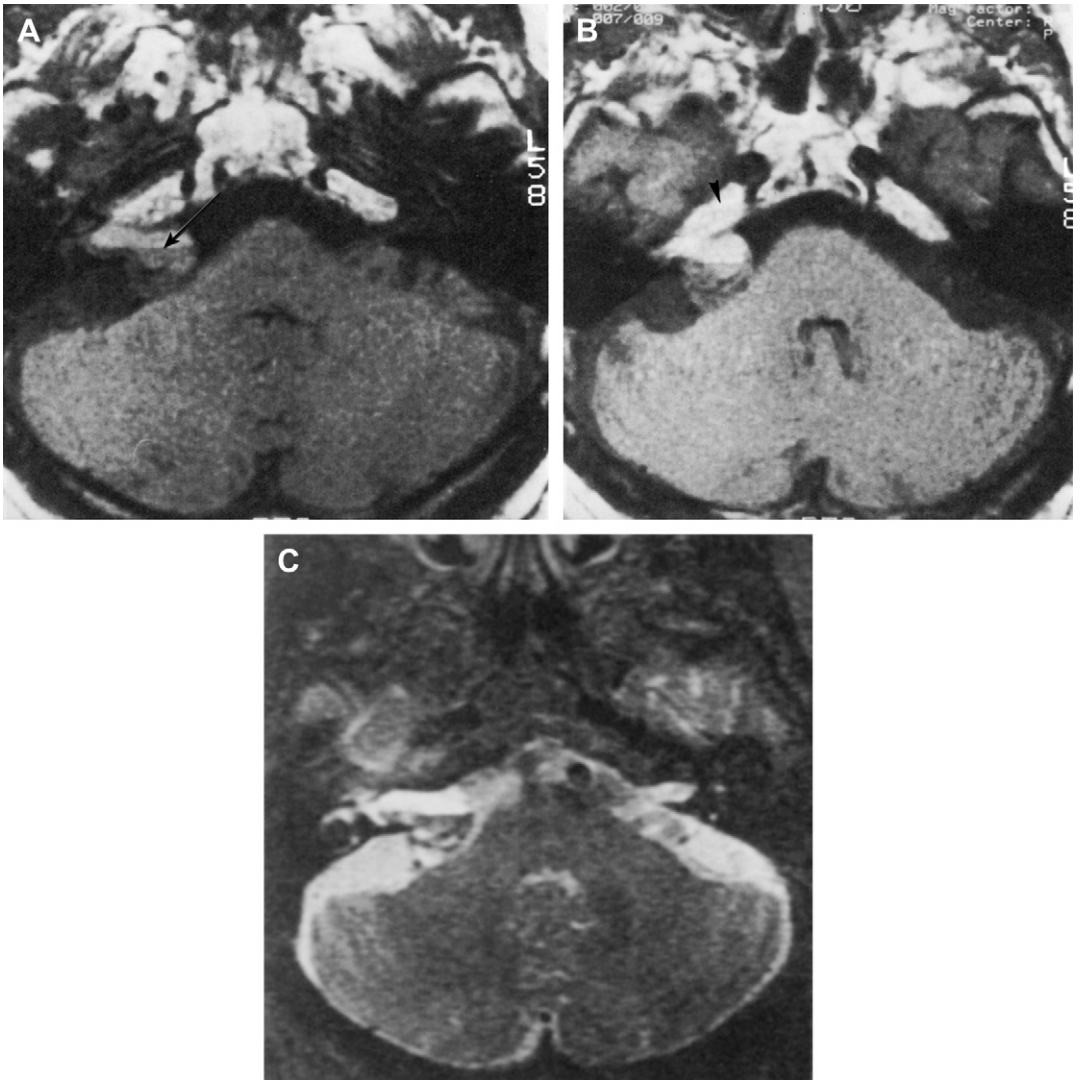

Fig. 5. Hemorrhage into an acoustic neuroma. This patient had an acoustic neuroma diagnosed previously. The patient had an acute hearing loss and underwent magnetic resonance imaging. At surgery the patient had a large hemorrhage into the acoustic neuroma. (*A*) T_1-weighted (TR 600/TE 20) image shows an acoustic neuroma on the right side with apparent fluid/fluid level (*arrow*). (*B*) T_1-weighted image slightly superior to that found in *A,* again shows fluid level representing layering of hemorrhage. Also note the bright signal (*arrowhead*) in the fat of the petrous apex. (*C*) T_2-weighted image showing even greater contrast between the fluid components of the hemorrhage.

the AN can develop completely within, completely outside, or partly inside, partly outside the canal. Most commonly, the lesion arises just inside the meatus and then grows out into the CPA cistern. Such a lesion is said to have both an intracanalicular and an extracanalicular component.

Intracanalicular tumor

As a tumor enlarges, several things happen that allow detection. First, the CSF, which usually is found within the canal, is replaced with soft tissue. This effect is difficult to see on CT but can be detected on MRI in many cases. Before the

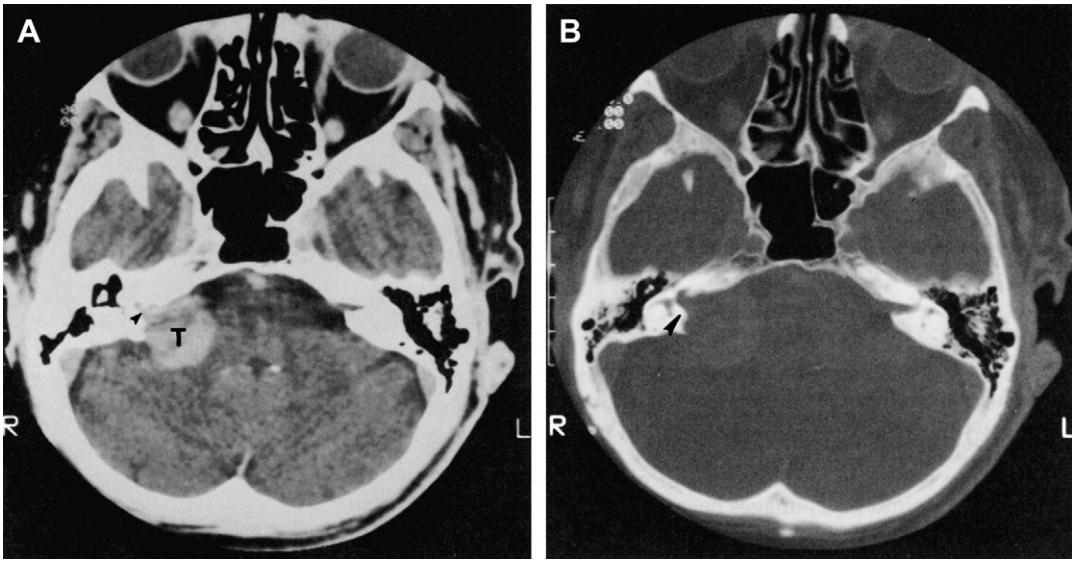

Fig. 6. (*A*) Acoustic neuroma with high resolution computed tomography with contrast. Soft tissue algorithms shows the tumor (T) protruding into the internal auditory canal (IAC) (*arrowhead*). (*B*) Bone algorithm shows the enlargement of the IAC (*arrowhead*).

widespread availability of gadolinium, many intracanalicular ANs were found on T_1 images because the tumor gave more signal than the CSF that should have been seen in the IAC if the patient were normal. Some radiologists preferred using extremely long TR sequences to make the CSF very bright so a small AN could be seen as a low-signal dark mass contrasted against the bright CSF (see Fig. 4B).

As the lesion grows within the canal, pressure is exerted on the walls of the canal, and a second

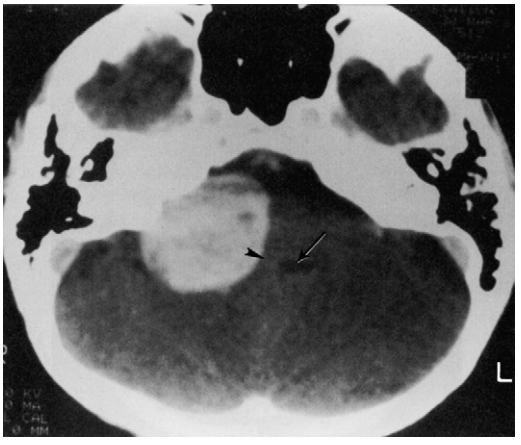

Fig. 7. Acoustic neuroma, enhanced computed tomography. Fairly homogeneous tumor pushing the pons, cerebellar peduncle, and fourth ventricle toward the contralateral side. Fourth ventricle (*arrow*), cerebellar peduncle (*arrowhead*).

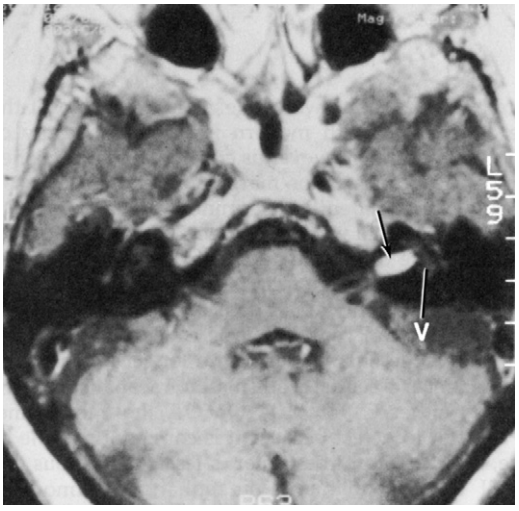

Fig. 8. Acoustic neuroma left side (T_1-weighted gadolinium-enhanced magnetic resonance image). Small enhancing neuroma (*arrow*) is seen filling the internal auditory canal but not protruding through the porus. Compare the enhancement of the neuroma to the nonenhancing fluid in the vestibule (V).

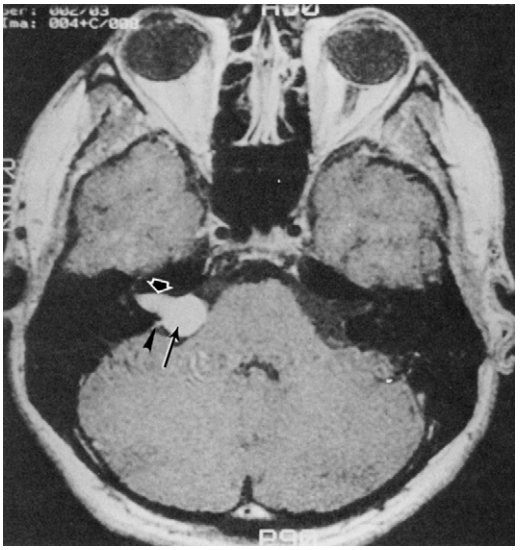

Fig. 9. Acoustic neuroma postgadolinium (T_1 weighted). The lesion (*arrow*) is seen protruding from the internal auditory canal. The intracanalicular portion (*open arrow*) is clearly identified contrasted against the extreme low signal of the petrous bone. Slight irregularity of the posterior edge of the tumor (*arrowhead*) is thought to represent slowly flowing blood in one of the branches of the petrosal vein.

effect can be detected. There is gradual enlargement of the canal. This secondary change was the basis of plain film and tomography screening of a decade ago. If significant asymmetry was seen, further, more invasive testing was done. This expansion of the canal can certainly be appreciated with modern imaging, especially on CT. The significance of the finding, however, is considerably diminished. Now the imaging shows the actual tumor margin rather than a secondary sign. Current imaging can confidently determine if an enlargement is due to a tumor or is simply a normal variation. The radiologist looks at the contents of the canal at the site of the enlargement (Fig. 11). If there is enhancement or soft tissue, the enlargement is the result of a tumor. But if the enlargement is filled with the typical density or signal intensity of CSF, the apparent enlargement can confidently be called a normal variation, and tumor as a cause of the enlargement is no longer a concern.

In our experience, essentially all small intracanalicular tumors exhibit enhancement on either CT or MRI. On CT, the enhancement may be obscured or difficult to detect because it is contiguous to the bone, which is very dense, and therefore the tumor is less conspicuous (see Fig. 11).

With MRI using gadolinium, the enhancing tumor is contrasted against the signal void of the cortical bone of the IAC. The bright signal is hard to miss (Fig. 12). The sensitivity of MRI in detecting intracanalicular tumors is therefore high. It is the resultant ability of MRI to exclude reliably small intracanalicular tumors that represents the real advantage of MRI over CT.

Extracanalicular tumor

As a lesion protrudes from the IAC into the CPA cistern, the tumor abuts the CSF and so becomes easily visible on CT as well as MRI. Even without contrast enhancement, most of these lesions are easily detectable on MRI. Once the lesion has grown beyond the plane of the porus, CT and MRI are about equal in the ability to detect the lesion. Either will detect almost every tumor.

The typical appearance of the mass growing into the CPA cistern is the mass tapering toward the porus (see Figs. 6A and 9). The angle made as the tumor meets the posterior surface of the petrous bone is acute rather than obtuse. These findings indicate that the site of origin is the IAC, and therefore the most likely diagnosis is AN.

Initially as the tumor grows into the CPA cistern, the advancing margin will be round until it encounters the brain stem. The level of the IAC is close to the great horizontal fissure of the cerebellum. Often the AN will push into the fissure. The tumor may appear to deform or flatten against the middle cerebellar peduncle (Fig. 13). This gives the appearance of a fairly rounded tumor with a flattened edge along the posteromedial aspect.

Further growth can push the pons and brain stem toward the contralateral side. As the shift of the brain stem occurs, the fourth ventricle can be deformed or compressed and obstructive hydrocephalus can occur (Fig. 14). Larger ANs can occasionally be associated with edema in the adjacent brain [20,21].

Extracanalicular tumor can also extend superiorly or interiorly. Superiorly the tumor can approach the fifth cranial nerve, which can easily be seen on axial or coronal MR images (Fig. 15) [22]. Further upward growth places the edge of the neuroma at the tentorial incisura. The superior extent is best appreciated on coronal

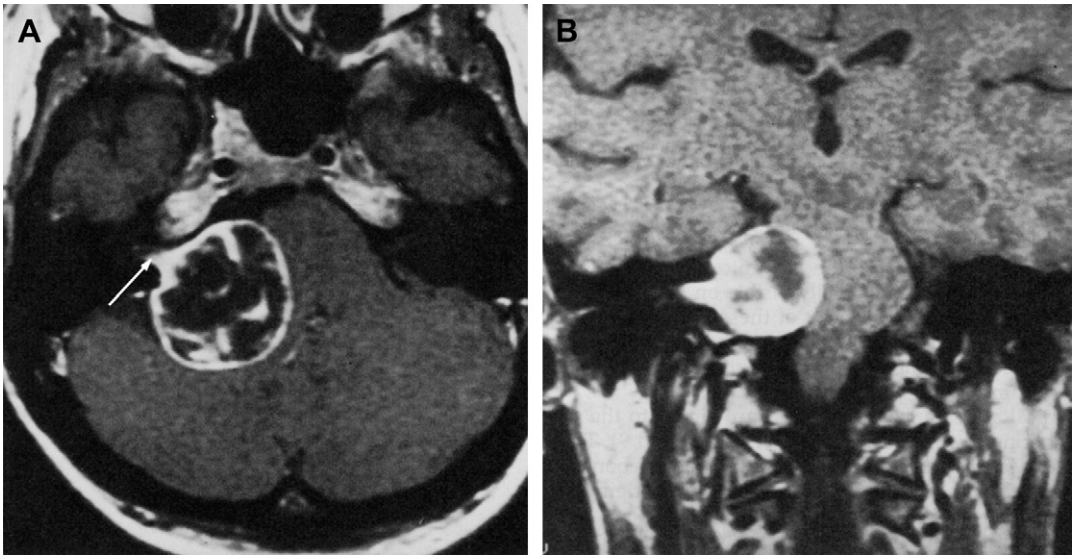

Fig. 10. (*A*) Partially enhancing acoustic neuroma in the CPA cistern. The edge of the tumor (*arrow*) protrudes into but does not completely fill the internal auditory canal. Note the many areas within the lesion that do not enhance and are of low signal. (*B*) Coronal image (same patient).

images but can be accurately estimated on axial images as well.

If the tumor has a component of growth in the caudal direction, the tumor is seen passing along the medulla and medial to the jugular foramen. The lesion should not obliterate the CSF signal (MRI) or density (CT) in the pars nervosa of the jugular foramen, nor does the tumor erode the mareins of the foramen (Fig. 16). If either of these findings is present, special care is warranted to be sure that the tumor is not actually arising in the jugular foramen rather than the IAC [9].

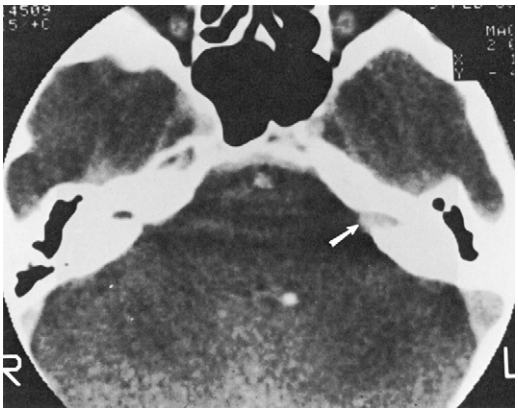

Fig. 11. Small acoustic neuroma on enhanced computed tomography. The edge of the tumor (*arrow*) is clearly seen. Compare the density within the canal with the cerebrospinal fluid density in the opposite canal.

Inferomedially directed growth follows the course of the seventh and eighth cranial nerves toward the root exit zone at the pontomedullary junction. The foramen of Luschka can be covered by the tumor. A small protrusion of choroid often passes through the foramen of Luschka into the lower CPA cistern. If this small bit of choroid is incorporated into the tumor, an arachnoid cyst can be formed in conjunction with the neuroma. Alternatively a portion of the CPA cistern can become isolated from the rest of the cisternal circulation, and a cyst or CSF collection can form posterolateral to the main part of the tumor. Cushing described such cysts or collections in a high percentage of the patients on whom he operated for AN (see Figs. 3A and 14). Currently these large cysts are less common probably because now lesions are confidently diagnosed and thus resected at a much earlier stage than they were in the early history of AN surgery.

Either CT or MRI can demonstrate these collections of CSF. CSF again has a very characteristic appearance. The fluid is dark on CT and homogeneous. There is little variation in the density within the fluid. On MRI, the CSF shows the characteristic low signal on T_1-weighted images and high signal on T_2-weighted images [10].

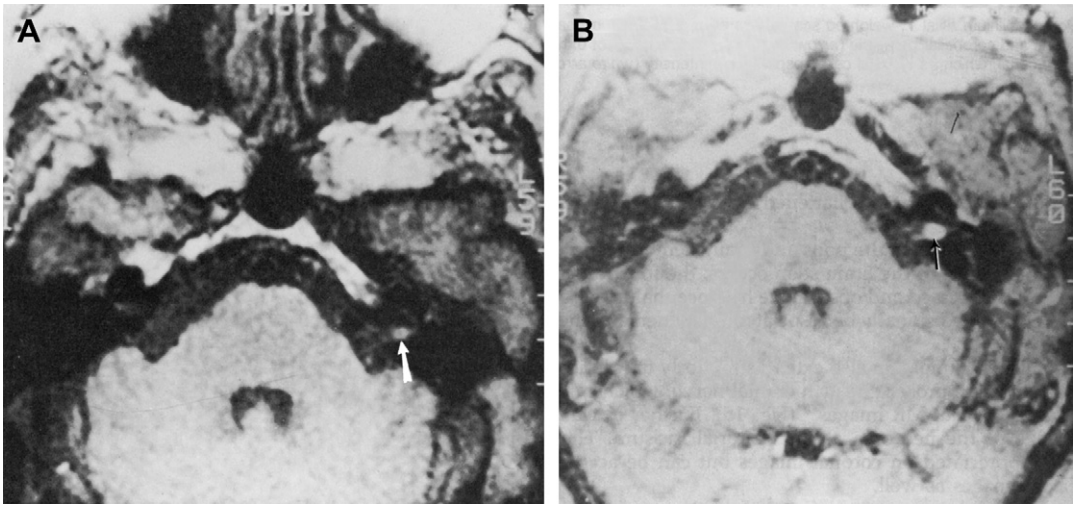

Fig. 12. (*A*) Pregadolinium T_1-weighted image shows a small acoustic neuroma (*arrow*) in the fundus of the left internal auditory canal (IAC). (*B*) Postgadolinium T_1-weighted image shows definite enhancement (*arrow*) of the rounded lesion in the IAC increasing the conspicuity of the lesion.

Most large ANs have both an intracanalicular and an extracanalicular component, but this is not always the case. Totally extracanalicular tumors can occur in two situations (see Fig. 13).

First, the Schwann cell–glial junction can actually be outside the meatus of the IAC. In this case, the tumor actually develops within the CPA cistern. The second postulated mechanism for occurrence of a totally extracanalicular AN is that a fairly firm or cellular tumor begins to develop in the medial part of the IAC. As it grows, the pressure begins to expand the canal. Eventually, however, the tumor develops enough leverage against the edge of the canal that the lesion actually pries or lifts itself out of the canal. In doing so, the tumor may actually avulse the nerve rootlets, leaving an "empty canal".

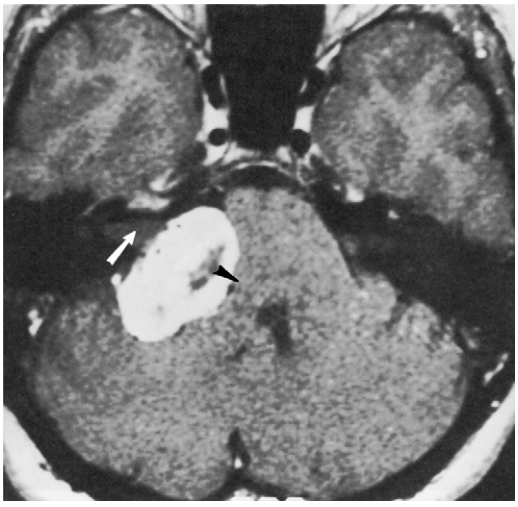

Fig. 13. Postgadolinium axial T_1-weighted scan shows an enhancing tumor at the porus pushing the pons and cerebellar peduncle (*arrowhead*). The lesion does not extend into the internal auditory canal, which has typical cerebrospinal fluid intensity (*white arrow*).

With either mechanism, the picture on CT or MRI is the same. There may be some erosion or expansion of the meatus of the IAC, but the intracanalicular region or especially the fundus is often relatively normal (see Fig. 13). The characteristic CSF density on CT or the characteristic CSF signal intensities on MRI can be seen in the depths of the canal. This is especially obvious on a long TR/long TE, heavily T_2-weighted MRI.

Rare occurrences

Most patients have a unilateral tumor and the tumor arises inside the IAC. There are rare exceptions. Bilateral ANs are seen in neurofibromatosis [23–27]. Because the diagnosis is not always known at the time of imaging, care should be taken to ensure that the opposite IAC is adequately visualized when an AN is first identified on one side (Fig. 17).

A much rarer occurrence is a neuroma originating within the otic Labyrinth. Only a few cases

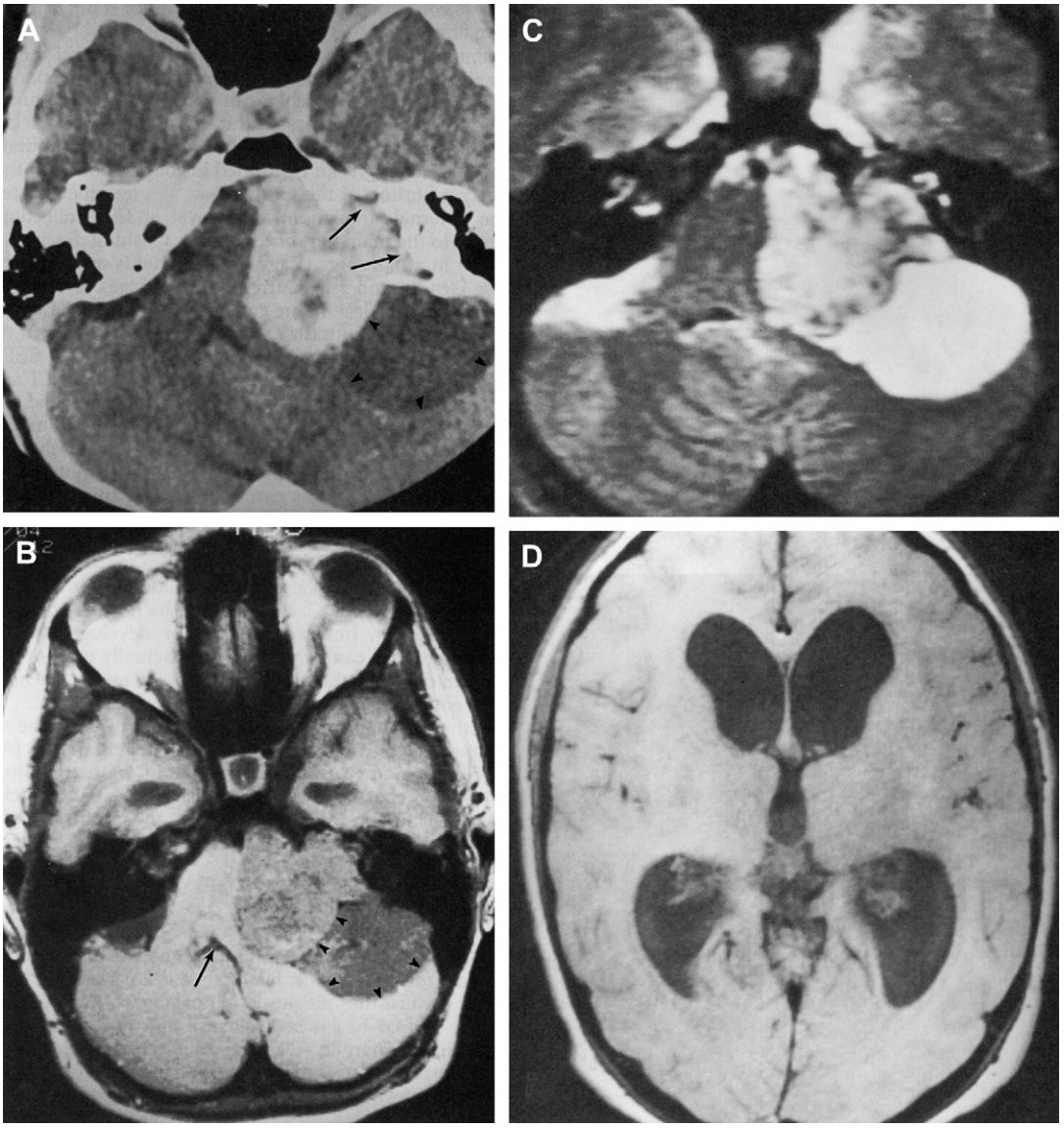

Fig. 14. Large acoustic neuroma with destructive enlargement of the internal auditory canal (IAC) and associated posterolateral arachnoid cyst. (*A*) There is destructive enlargement of the IAC (*arrows*). There is a large arachnoid cyst posterolaterally (*arrowheads*). (*B*) Axial T_1-weighted (spin echo 500/20) image. The trapped arachnoid cyst (*arrowheads*) is seen posterolateral to the tumor on this unenhanced image. The fourth ventricle (*arrow*) is deviated. (*C*) T_2-weighted image (SE 2500/75). The posterolateral component has the same brightening as cerebrospinal fluid. (*D*) Axial T_1-weighted slice through the upper brain shows hydrocephalus due to the compression of the fourth ventricle.

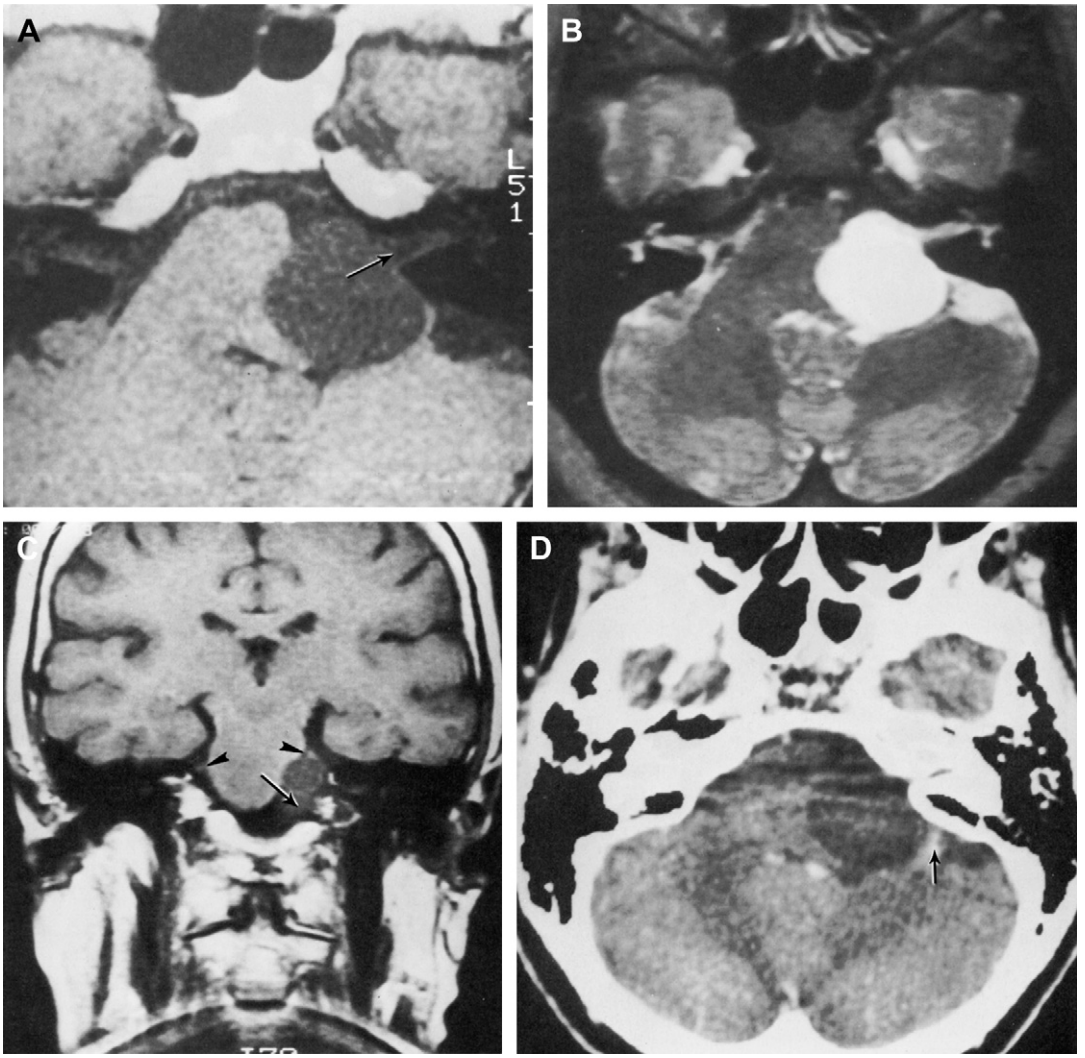

Fig. 15. Cystic neurilemoma of CPA cistern. Lesion probably arising from the glossopharyngeal nerve. (*A*) T_1-weighted image (no gadolinium). The lesion is seen in the CPA cistern pushing the brain stem and pons toward the right. The lesion protrudes into the porus but does not fill the internal auditory canal. Edge of lesion (arrow). (*B*) T_2-weighted image shows high signal in the apparently cystic abnormality. (*C*) Coronal T_1-weighted image. The lesion could be followed to the pars nervosa interiorly (*arrow*). The lesion pushed the trigeminal nerve (*arrowhead on right*) superiorly. Compare with trigeminal nerve on the opposite side (*arrowhead*). (*D*) Axial computed tomography scan post-contrast. Petrosal vein tributaries are pushed posteriorly (*arrow*) and the lesion does not enhance. This lesion was attached to the glossopharyngeal nerve at surgery.

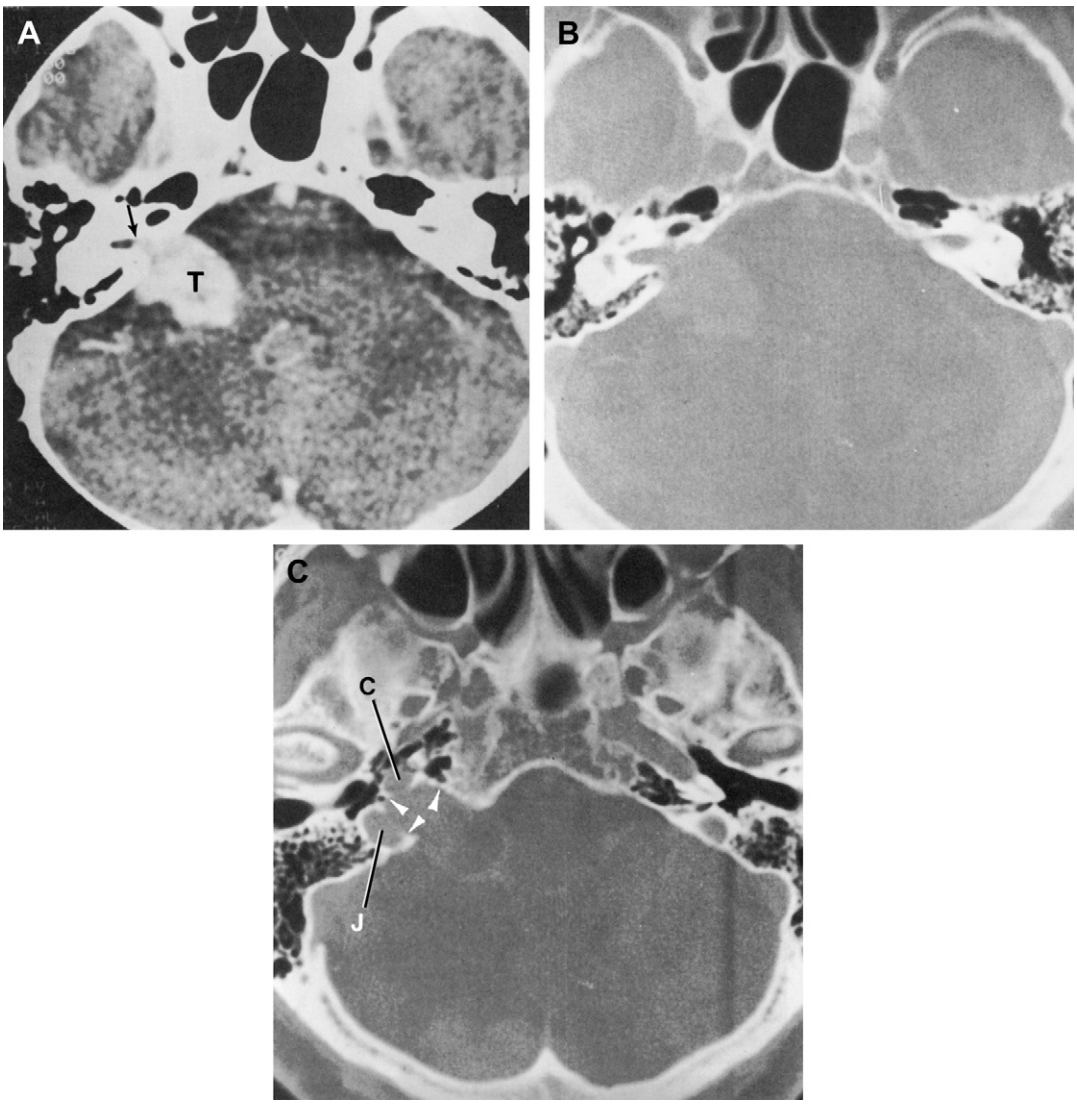

Fig. 16. Glossopharyngeal neurilemoma protruding into CPA cistern. (*A*) Tumor is seen at the level of the internal auditory canal (IAC) and protrudes into the porus (*arrow*). T, tumor. (*B*) On a bone algorithm there is no enlargement of the IAC. There is minimal erosion of the porus. (*C*) Inferior slice bone algorithm. There is enlargement of the pars nervosa (*arrowheads*) indicating the origin of the lesion. J, jugular fossa; C, carotid canal.

have been reported. These would be detected as enhancement within the confines of the labyrinth. On CT, there may be some bone expansion or erosion.

Differential diagnosis

The appearance of an AN is usually characteristic enough that the diagnosis can be made with confidence, and the possibility that the lesion is something else is remote. There are certainly other tumors, however, that occur in the region of the IAC and the CPA cistern that can be confused with ANs [11,49]. Probably more important are certain inflammatory conditions that can mimic tumors.

Nontumoral enhancement

The gadolinium-enhanced MRI scan has increased our ability to exclude an AN reliably.

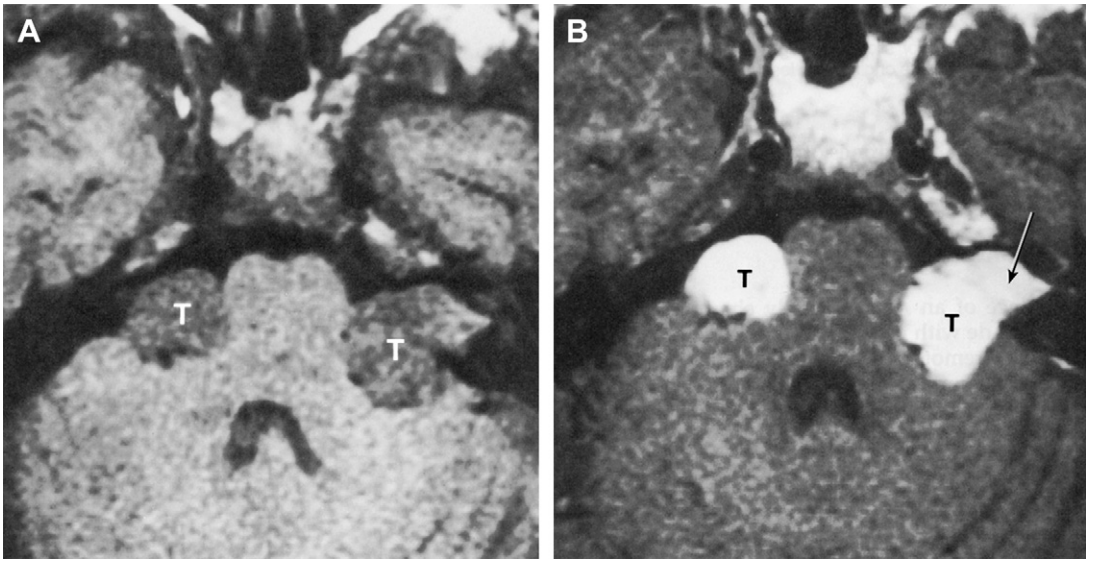

Fig. 17. (*A*) Bilateral acoustic neuromas. T_1-weighted image without contrast shows bilateral tumors (T). (*B*) Axial T_1-weighted image after gadolinium shows enhancement of the tumors bilaterally. Note the intracanalicular portion on the right side (*arrow*). The slice is too high to see the intracanalicular portion on the left.

Subtle enhancement in the IAC is dramatically obvious in even tiny tumors. Not everything that enhances, however, is a tumor. Indeed not everything that enhances is abnormal.

Depending on the time relationship between contrast injection and imaging, small vessels, especially those with slow flow, can appear to "light up." Even areas of vascular anastomosis can enhance. An example of this phenomenon is the region of the geniculate ganglion, where a small amount of enhancement is often seen in patients without any symptoms. Occasionally there is a small amount of enhancement within the IAC itself. This enhancement may represent a small vessel but can be of concern if seen on the side of symptomatology [29].

Recently attention has been focused on enhancing inflammatory nontumoral conditions (Fig. 18). This phenomenon was identified in Bell's palsy, in which definite enhancement was noted to occur in the facial nerve canal traversing the temporal bone [30,31]. The enhancement could involve the entire nerve or be more localized to the region of the geniculate ganglion. Because of the typical presentation of Bell's palsy, it was quickly realized that this enhancement did not represent a tumor. CT would show a normal-sized facial nerve canal, thus making a tumor unlikely. As the symptoms wane, the enhancement has been reported to decrease, although resolution of the radiologic finding may lag behind clinical resolution of symptoms [31].

Patients with acute inflammation of the labyrinth or the nerves within the IAC can exhibit similar enhancement but now in the region where the finding can be confused with an AN (see Fig. 18). Investigators have shown the increased signal to correlate with the rapid onset of symptoms, suggesting a viral infection [32,33].

It should also be remembered that not everything that is bright on a T_1-weighted image represents enhancement. Hemorrhage at various stages and even fluid with a high protein content can look exactly like enhancement (Figs. 19 and 20). One can easily determine if high signal represents enhancement by comparing the postgadolinium scan with a non–contrast enhanced image, but this is not always available [34]. In ambiguous cases, it may be helpful to repeat a scan after several days when the gadolinium has cleared.

Caution should therefore be exercised when a small amount of enhancement is seen inside the canal on MRI. This is especially true if there is no enlargement of the canal that correlates with the area that is enhancing or if the enhancement does not have a clearly defined edge to suggest a tumor. In questionable cases, following the clinical course and reimaging the patient after a short time interval is appropriate.

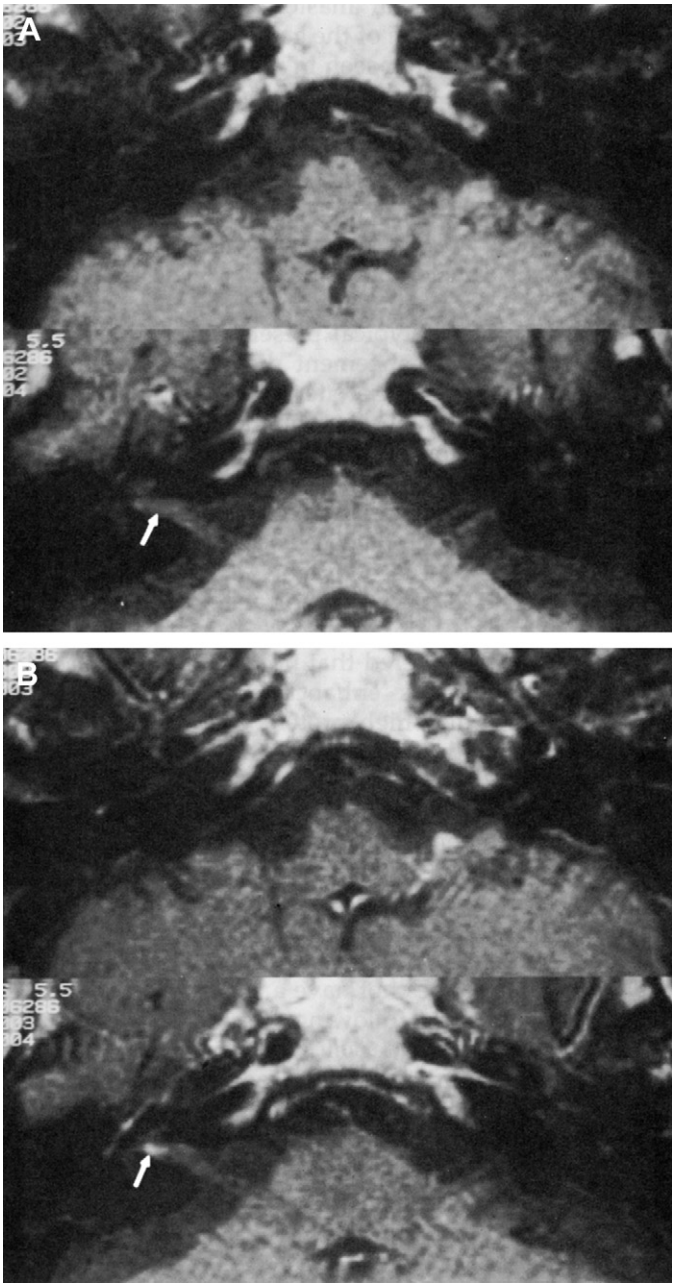

Fig. 18. Bell's palsy. (*A*) Axial T_1-weighted image pregadolinium shows slight increased signal in the internal auditory canal (IAC) (*white arrow*). (*B*) Postgadolinium image shows enhancement in the fundus of the IAC (*white arrow*). The enhancement is irregular and there is no obvious tumor edge. (*C*) Coronal postgadolinium image shows enhancement of the two dots representing the labyrinthine and tympanic segment of the facial nerve canal (*arrow*). Compare with opposite side (*open arrow*). (*D*) Slightly posterior slice shows some enhancement in the IAC (*open arrow*). Trigeminal nerve seen in cross section (*arrow*).

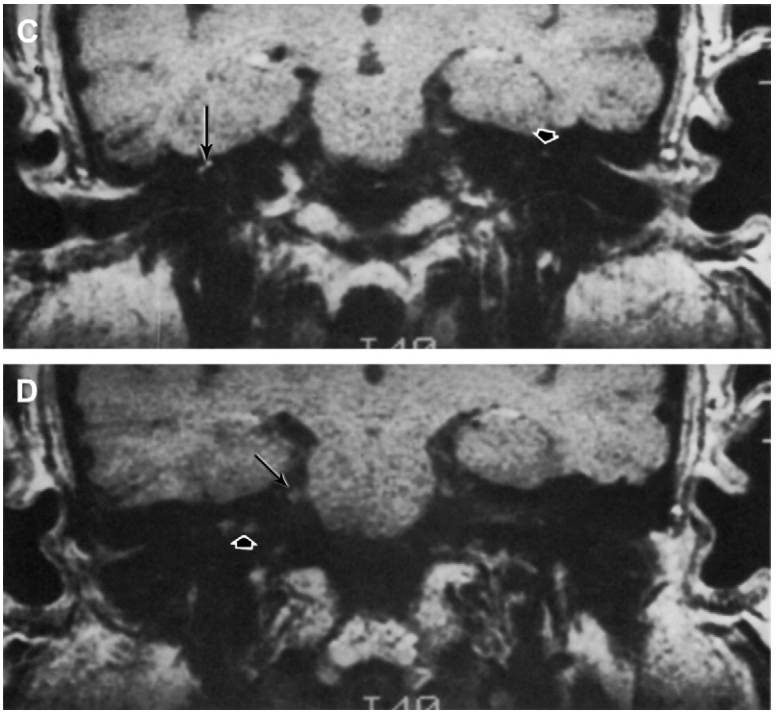

Fig. 18 (*continued*)

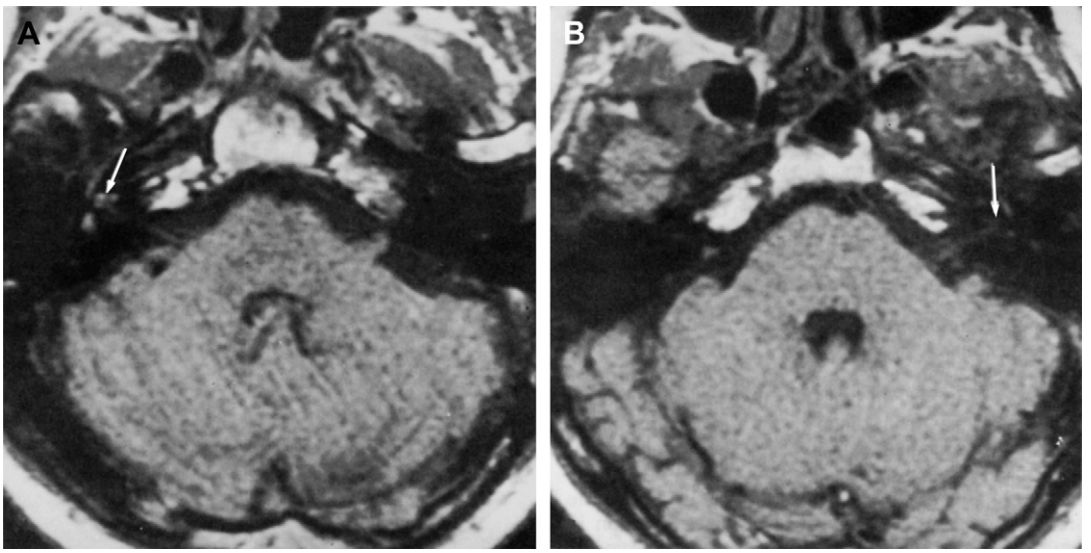

Fig. 19. Patient with sudden hearing loss. (*A*) Precontrast study shows increased signal in the cochlea (*arrow*) and vestibule. Compare with lower signal from the normal cochlea in *B*. (*B*) Image through the cochlea on the opposite side shows normal low signal in the labyrinth.

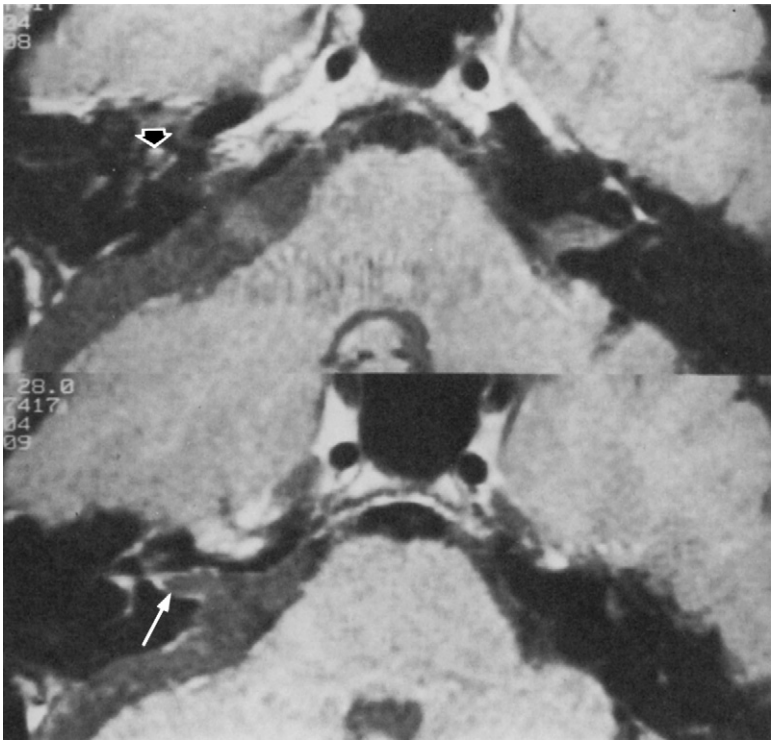

Fig. 20. Postresection postgadolinium T_1-weighted magnetic resonance imaging scan shows enhancement along the wall of the internal auditory canal (*arrow*) with some increased signal in the cochlea (*open arrow*). The increased signal in the cochlea could be a small amount of blood. This increased signal represented a change from the preoperative examination.

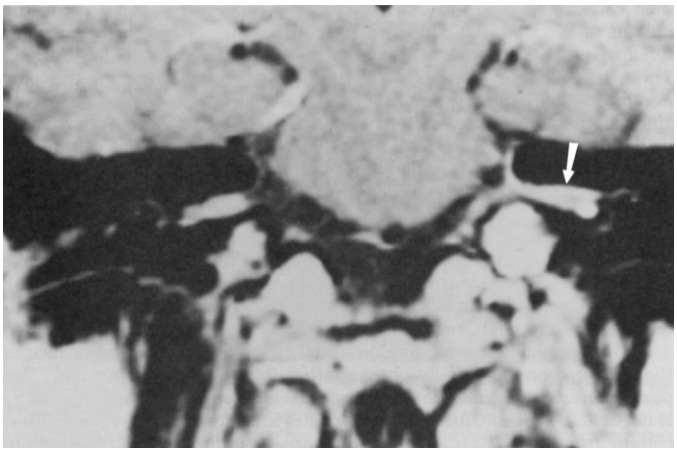

Fig. 21. Sarcoid involving the internal auditory canal (IAC). T_1-weighted image with gadolinium shows enhancement (*arrow*) in both IACs. There is no widening of the canal. (*Courtesy of* Dr. Alexander Marks.)

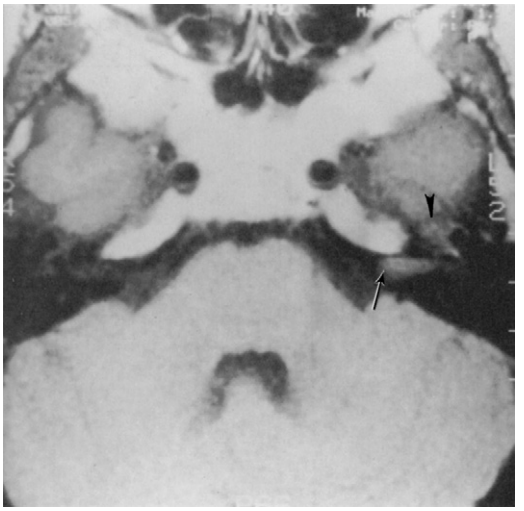

Fig. 22. Facial nerve neuroma shows an intracanalicular tumor (*arrow*) that is indistinguishable from an acoustic neuroma. There is a small lesion, however, in the geniculate (*arrowhead*) indicating the true nature of the lesion. Compare with opposite side.

Other types of inflammation have been reported to cause enhancement in the canal extending into the CPA cistern. Sarcoid and syphilis can cause enhancement that appears to follow the nerve and closely approximates the appearance of an AN (Fig. 21) [35]. Often the margin is unsharp rather than smooth, giving a clue that the lesion is not a nerve sheath tumor.

Tumors and cysts

AN is certainly the most common tumor of the IAC and CPA cistern. There are many other tumors that arise in this location and can occasionally be confused with AN. These include facial nerve sheath tumors, meningiomas, epidermoids, various intra-axial tumors, and a variety of extremely rare lesions [7,9,11,36,37]. Nerve sheath tumors developing from cranial nerve V or cranial nerves IX, X, or XI can grow into the region of the IAC. On CT, an aneurysm can look just like a seventh cranial nerve sheath tumor. Metastasis from distant primaries can involve the nerves in the IAC and thus mimic an AN on imaging. Leukemia has been reported to infiltrate along the nerves and look like an AN on MRI.

A facial nerve sheath tumor that arises totally inside the IAC would be impossible to differentiate from an AN based only on imaging. Like AN, the tumor arising from the sheath of the cranial nerve VII will enlarge the IAC and will enhance on either CT or MRI. Facial paralysis is usually but not always present. In most cases, the facial neurilemoma can be followed into the

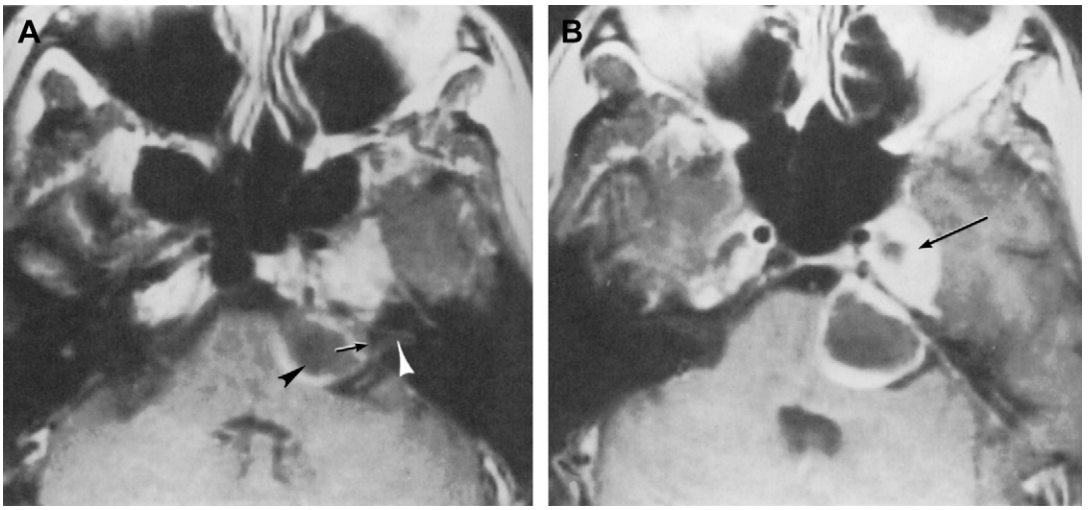

Fig. 23. (*A*) T_1-weighted postgadolinium magnetic resonance image. Trigeminal neuroma. Lesion in the CPA cistern shows a low density cystic center (*black arrowhead*). The lesion extends into the porus (*arrow*) but does not involve the deep fundus (*white arrowhead*) of the internal auditory canal. (*B*) T_1-weighted postgadolinium image. Slightly higher slice shows the lesion in the CPA cistern protruding into Meckel's cave (*arrow*) indicating the identity of the tumor.

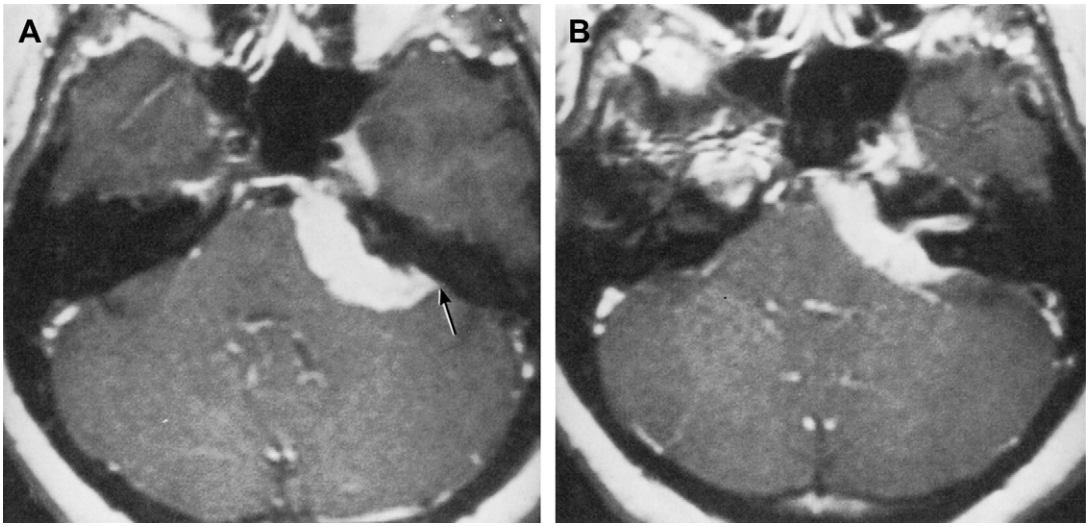

Fig. 24. (*A*) Meningioma of the posterior wall. An enhancing mass lesion is seen forming an obtuse angle (*arrow*) with the posterior wall of the petrous bone. (*B*) Enhancing lesion covers the internal auditory canal (IAC) but the tapering edge suggests the identity. There is enhancement indicating involvement of the IAC.

labyrinthine segment of the fallopian canal, and so the identity is determined (Fig. 22) [30].

Nerve sheath tumors developing from the nerves of the jugular foramen can grow up to the CPA cistern and can even seem to erode the meatus of the IAC (see Fig. 16). Indeed they can present with symptoms relating to the eighth cranial nerve rather than the actual nerve of origin. These lesions can be expected to erode the bony margin of the pars nervosa of the jugular foramen and can often be followed extracranially along a course just posterior to the internal carotid artery immediately below the skull base. For this

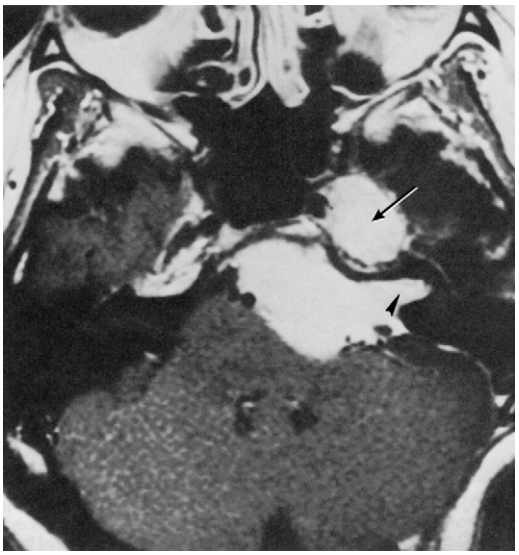

Fig. 25. Meningioma of the posterior and middle cranial fossa. T_1-weighted axial image postgadolinium shows the lesion in the posterior fossa protruding into the internal auditory canal (*arrowhead*). The lesion has a definite involvement in Meckel's cave (*arrow*) that should not occur with an acoustic neuroma.

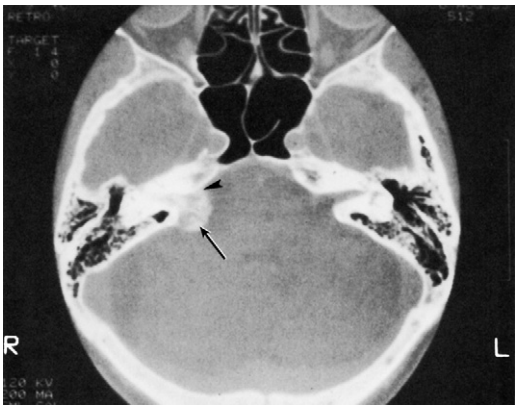

Fig. 26. Meningioma of the internal auditory canal (IAC). Computed tomography scan on a bone algorithm shows a calcified mass protruding from the IAC (arrow). Because this lesion arises from the IAC the junction between the lesion and the posterior wall of the petrous bone is more acute (*arrowhead*).

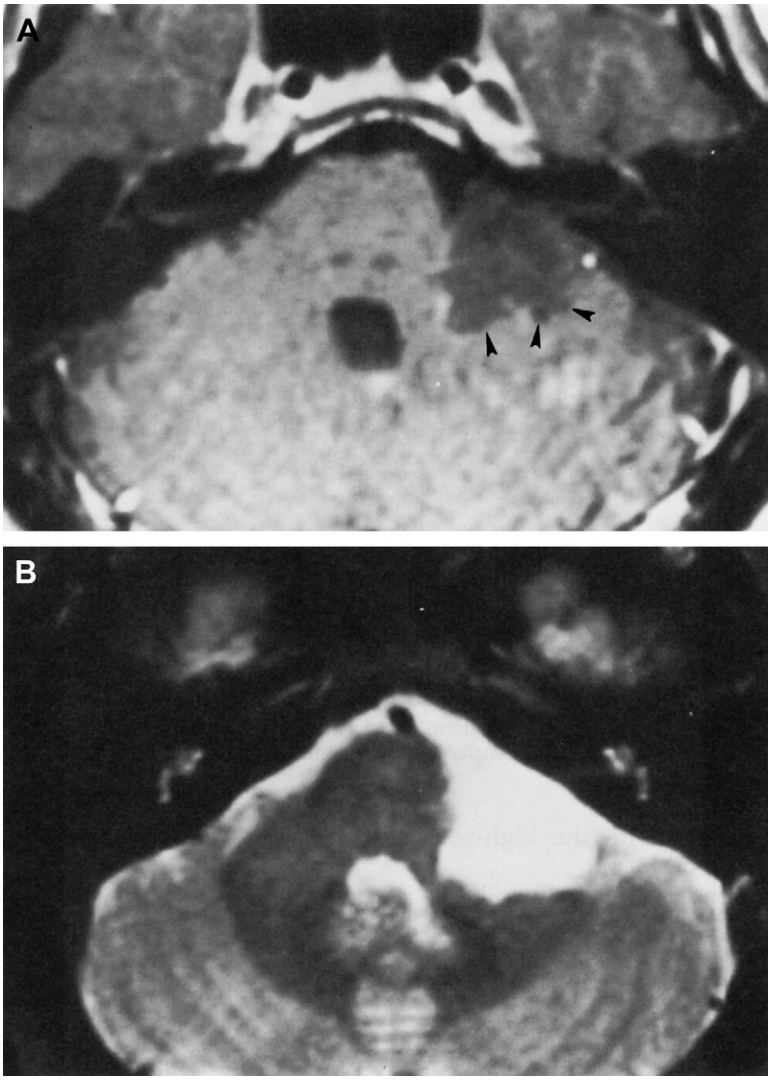

Fig. 27. (*A*) Epidermoid of the CPA cistern. T_1-weighted image. The lesion has slightly more signal than the cerebrospinal fluid. The lesion has an irregular margin as it extends into irregularities of the cerebellum (*arrowheads*). (*B*) T_2-weighted image shows the lesion to have very bright signal.

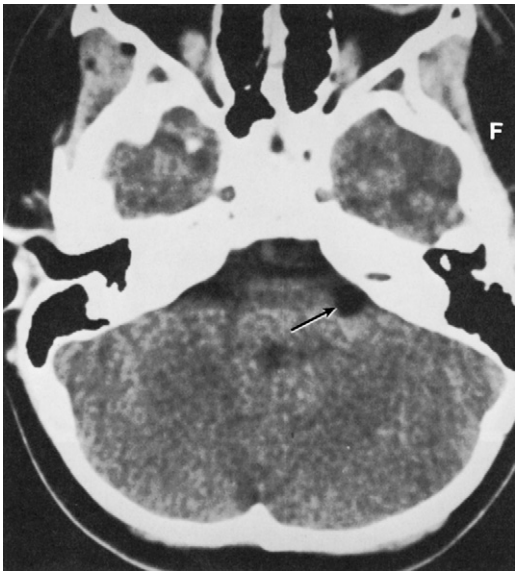

Fig. 28. Lipoma of the CPA cistern. Small lesion with extremely low density on an unenhanced scan (*arrow*). The density reading was the same as the subcutaneous fat (*F*).

reason, the imaging study should define the inferior extent of a presumed AN. For a similar reason, the superior margin should be found, thus making sure that the lesion is not arising from Meckel's cave and the fifth cranial nerve (Fig. 23).

Meningiomas can usually be differentiated from an AN [9,37a]. The classic description states that a meningioma has a flatter, more extensive attachment to the posterior surface of the petrous bone (Figs. 24 and 25) [38]. In other words, the tumor covers a wider region rather than being localized to the immediate region of the IAC [39].

The margin that a meningioma makes with the posterior surface of the petrous bone is usually obtuse rather than acute as in an AN. This particular finding is reliable when present. The presence of an acute angle is not actually specific for an AN but rather indicates only that the lesion is coming from the IAC. If a meningioma arises within the IAC, [39] this lesion can be expected to make an acute angle with the posterior surface of the petrous bone (Fig. 26).

The dura close to the margin of a meningioma can enhance for a variable distance away from the apparent edge of the tumor. This finding suggests the diagnosis of meningioma rather than AN.

Meningiomas can calcify and frequently cause hyperostosis of the contiguous bone. Either of these findings should be considered a strong indicator that the tumor is not an AN but rather a meningioma. Hyperostosis is said to be less common in those meningiomas arising along the

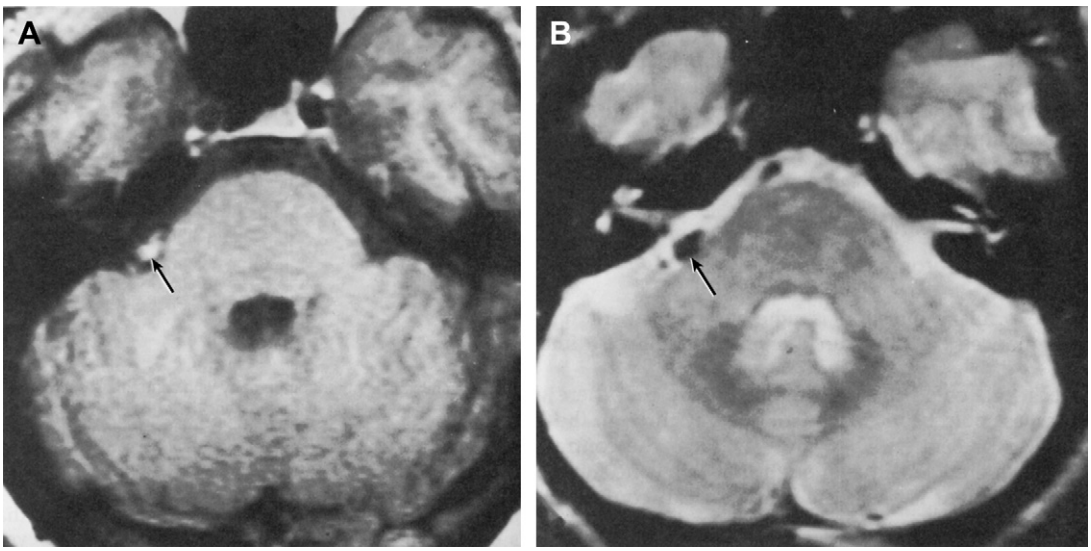

Fig. 29. Lipoma of the CPA cistern. (*A*) T_1-weighted image without contrast shows a small bright mass (*arrow*). (*B*) On the T_2-weighted image, the lesion becomes dark, which is characteristic of fat.

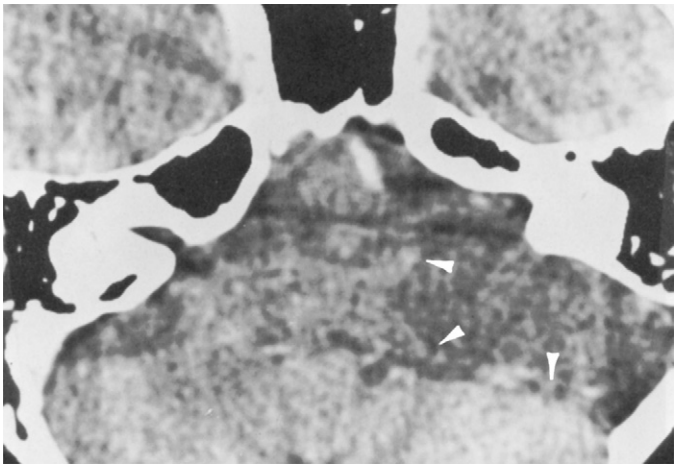

Fig. 30. Arachnoid cyst. Computed tomography with contrast. Cerebrospinal fluid density lesion shows mass effect by pushing the cerebellum and brain stem (*arrowheads*). (*From* Lo WWM: The temporal bone. In: Som PM, Bergron RT, editors. Head and Neck Imaging, edition 2. Mosby-Yearbook; 1991; with permission.)

posterior border of the petrous bone [38] than in other meningiomas but when present is suggestive of the diagnosis.

Hemangiomas arise in the IAC as well as in the region of the facial nerve canal [40,41]. These small lesions can look just like an AN, and this diagnosis should be considered when a small area of enhancement is seen in the IAC.

Lipomas and epidermoids have characteristic appearances on both CT and MRI and should not be confused with an eighth cranial nerve tumor. An epidermoid is expected to be low signal on T_1-weighted images and high signal on T_2-weighted images (Fig. 27). On CT, the lesion may have the same density as CSF. Rarely an epidermoid can be dense on CT [42]. An epidermoid will not

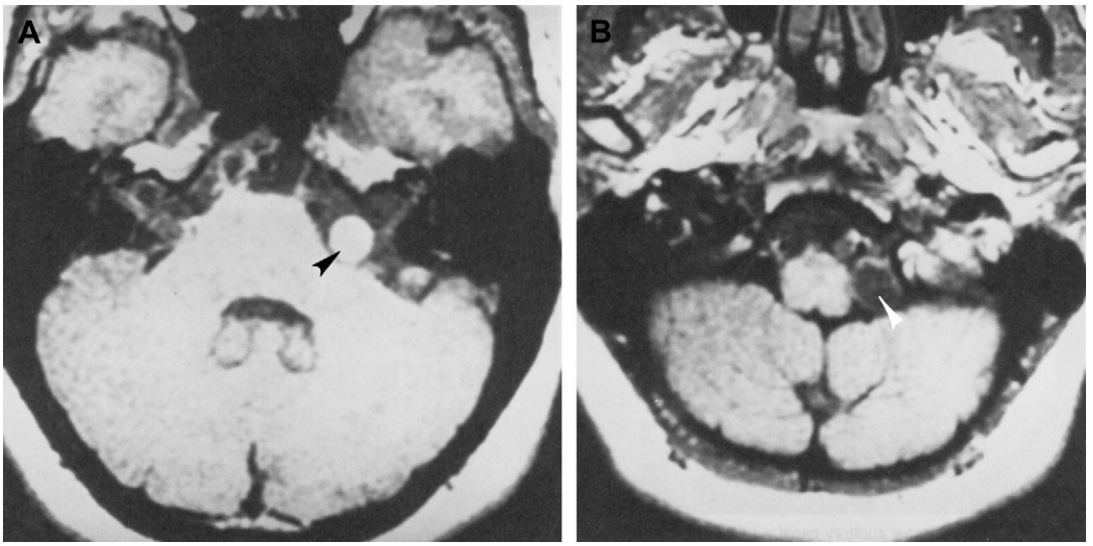

Fig. 31. Cysticercosis. (*A*) Noncontrast (SE 733/20) image shows high signal mass (*arrowhead*) in the CPA cistern. (*B*) Scan at the lower level shows another more typical cyst. Note that at this level a distinct wall can be identified. There is a small focus of signal from within the cyst (*arrowhead*). This may represent a scolex within the cyst.

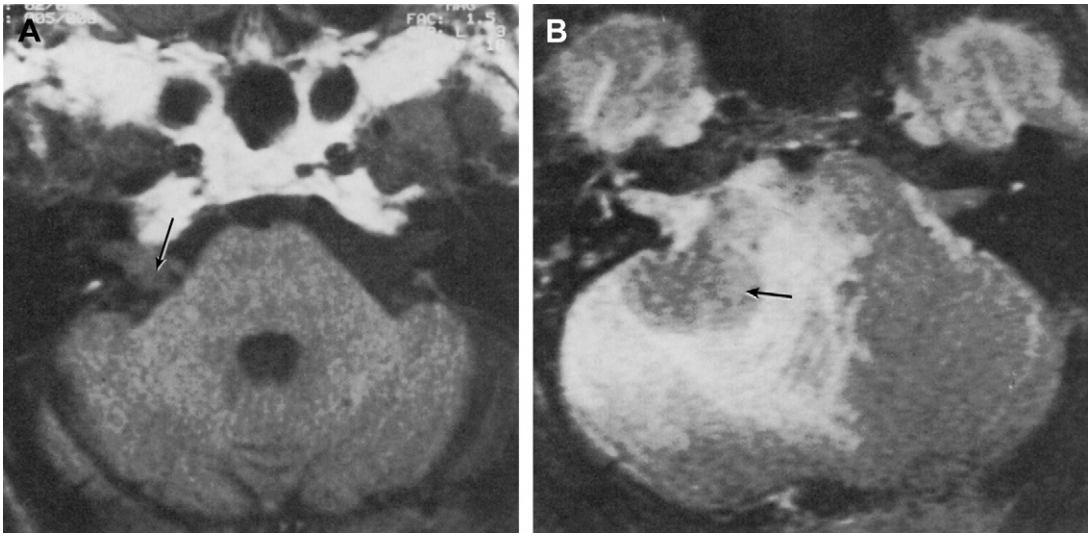

Fig. 32. Metastases to the internal auditory canal with facial nerve paralysis and hearing loss. (*A*) T_1-weighted image without gadolinium shows a soft tissue mass (*arrow*) filling the porus and protruding into the CPA cistern (*arrow*). Computed tomography scan showed slight enlargement of the facial nerve canal (not shown). (*B*) Two months later there is a considerable increase in symptoms. The mass (*arrow*) has increased in size. There is shift of the brain stem and considerable edema in the brain contiguous with the lesion.

enhance on either CT or MRI. A lipoma is high signal on T_1 without contrast enhancement and low signal on T_2, and on CT it will have a characteristic low (fat) density (Figs. 28 and 29).

Arachnoid cysts can occur in the posterior fossa either as an isolated finding or in association with an AN. An isolated arachnoid cyst may have an appearance much like that of an epidermoid. It will be the density of CSF on CT and behave like CSF on MRI (dark on T_1 and bright on T_2) (Fig. 30). Again there should be no enhancement on either CT or MRI.

Cysticercosis is a rare cause of a cystic abnormality in the cerebellopontine angle cistern (Fig. 31) [43,44]. The abnormality may be seen as a discrete cyst or may be irregular with the cysts forming conglomerations that cannot be clearly separated from the contiguous CSF spaces. The signal on MRI and the density on CT closely mimic CSF. This diagnosis should be considered in regions where this disease is common.

Metastasis affecting cranial nerves VII and VIII usually involves the bone first and extends into the region of the canal secondarily. Occasionally a metastasis can reach the IAC by direct hematogenous (Fig. 32) or even intrathecal spread (Fig. 33). This infrequent occurrence can be impossible to differentiate from AN, especially

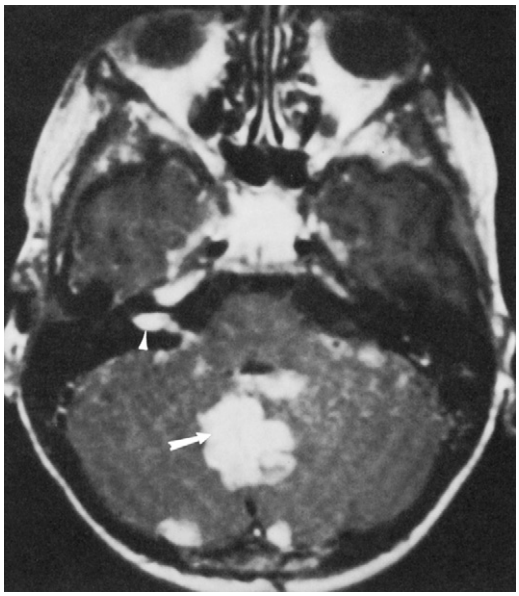

Fig. 33. Subarachnoid metastases from primitive neuroectodermal tumor. Axial postcontrast magnetic resonance images (SE 500/20). There is an enhancing mass in the cerebellar vermis (*arrow*). There are multiple subarachnoid metastases including one in the right internal auditory canal (*arrowhead*).

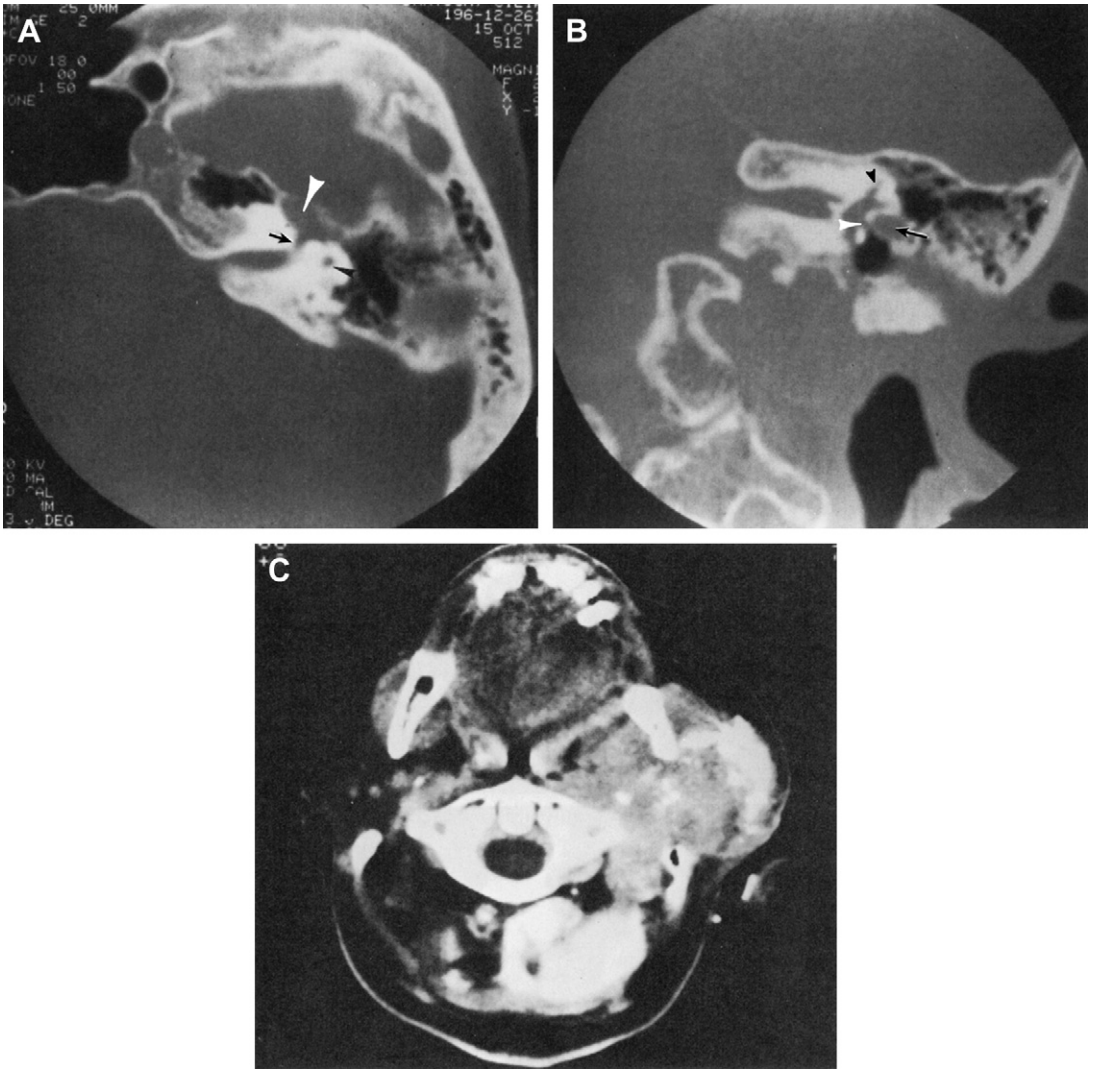

Fig. 34. Perineural extension along the facial nerve canal. Patient has parotid mass and facial paralysis. (*A*) There is enlargement of the geniculate ganglion (*white arrowhead*) with slight enlargement of the labyrinthine segment of the facial nerve canal (*arrow*). Superior semicircular canal (*black arrowhead*). (*B*) Coronal image shows enlargement of the tympanic segment of the facial nerve canal (*arrow*). Normal structures; oval window (*white arrowhead*), superior semicircular canal (*black arrowhead*). (*C*) Computed tomography sialogram. Inferior slice shows a large tumor in the parotid gland.

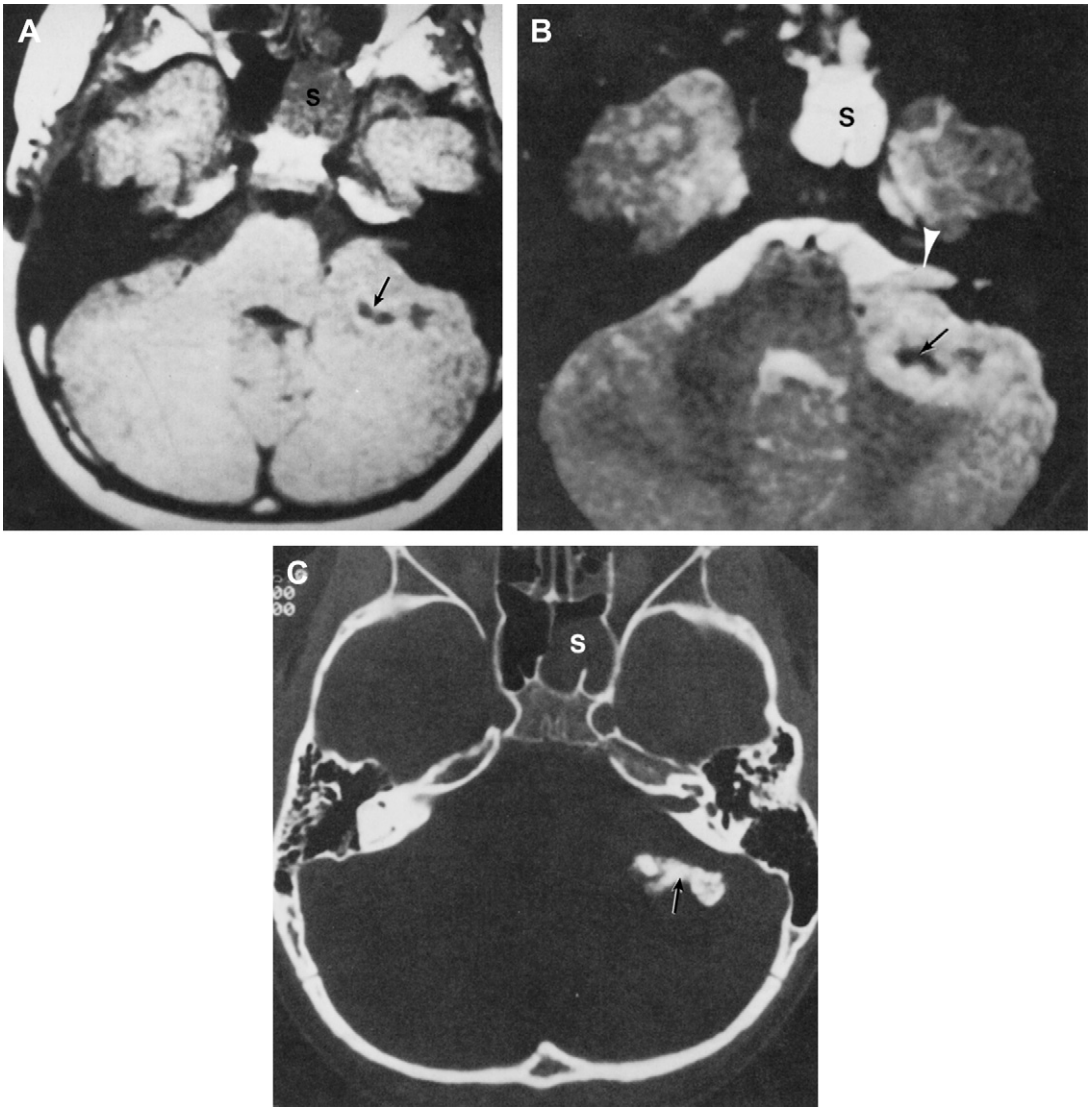

Fig. 35. Cerebellar astrocytoma with extension into the internal auditory canal in a 7-year-old boy. (*A*) Axial T_1-weighted image shows lesion in the CPA cistern. The low signal area (*arrow*) does not represent fluid but calcium. (*B*) T_2-weighted image again shows the low signal of the calcified region (*arrow*). The lesion protrudes into the internal auditory canal (*arrowhead*). (*C*) Computed tomography demonstrates calcification (*arrow*). Note the secretions (S) in the left sphenoid sinus.

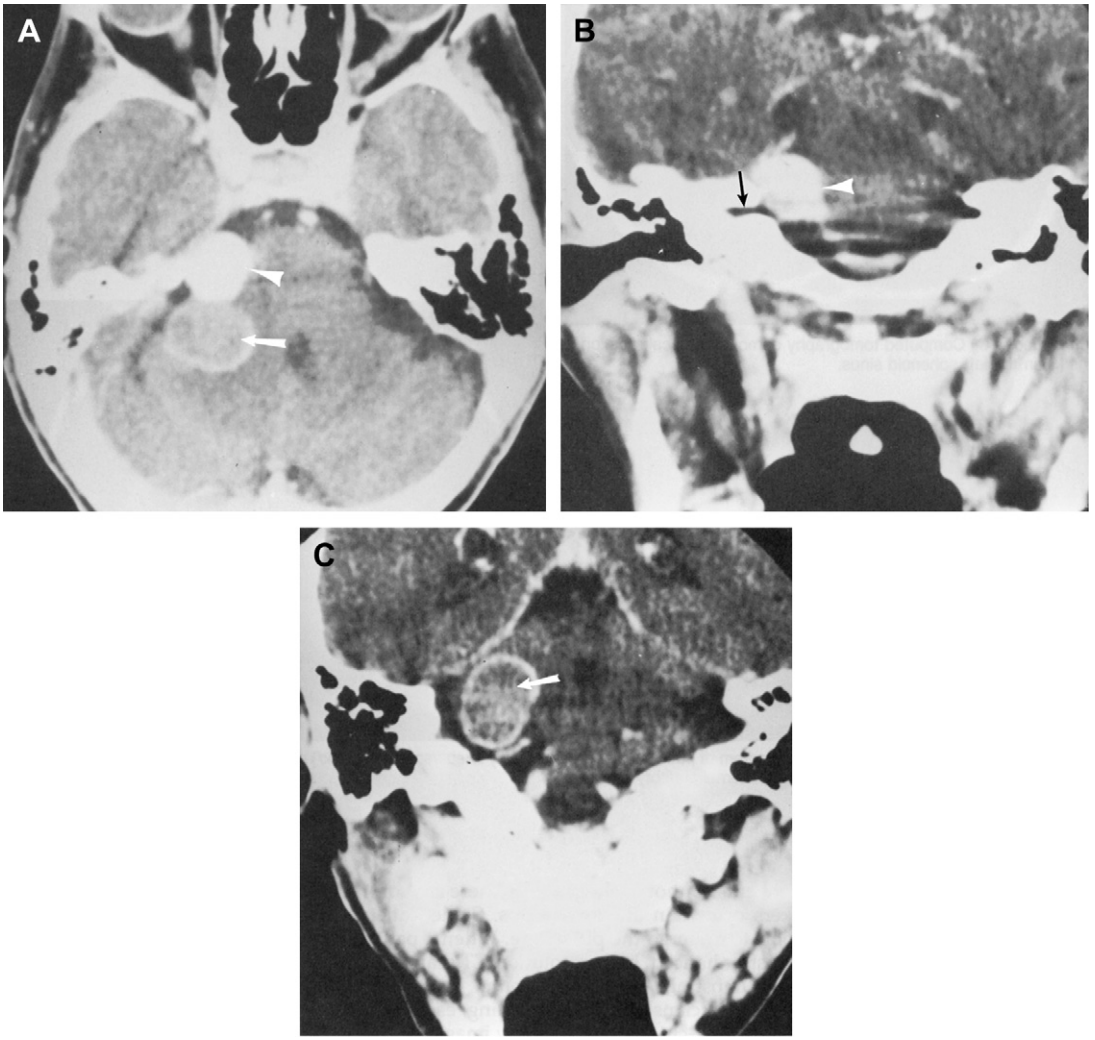

Fig. 36. (*A*) Partially thrombosed aneurysm of the vertebral artery. "Mass" in the CPA cistern is bilobed. The anterior portion (*arrowhead*) opacifies on venous injection of contrast. The posterior portion (*arrow*) does not opacify indicating thrombus. (*B*) Coronal image through the anterior portion of the mass shows enhancement (*arrowhead*). Note that the mass does not protrude into the internal auditory canal (*arrow*). (*C*) Posterior slice shows the thrombosed portion of the aneurysm (*arrow*).

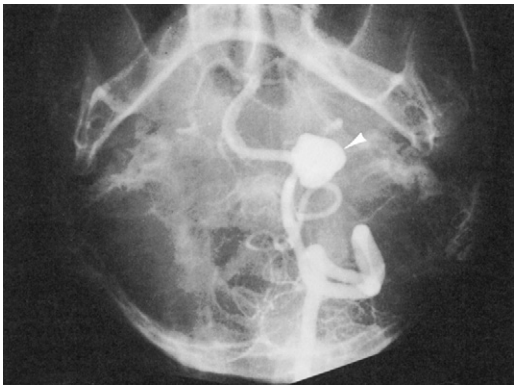

Fig. 37. Arteriogram of patient with vertebral artery aneurysm (*arrowhead*) at the approximate level of the internal auditory canal.

if the patient is not known to have a primary malignancy. Rapid growth may suggest this diagnosis.

Metastasis can also reach the IAC by spreading along the facial nerve. This so-called perineural spread is from malignancy of the parotid gland, usually an adenoid cystic carcinoma (Fig. 34). This should not be a diagnostic problem because the primary tumor is obvious either on the images or to palpation. The tumor can be followed along the nerve, enlarging the facial nerve canal.

Tumors arising in the brain stem or cerebellum can grow out into the CPA cistern (Fig. 35). In the past, differentiation from AN could be difficult but with the high-resolution imaging available today, this is seldom a problem.

A choroid plexus papilloma can arise in the fourth ventricle and extend through the foramen of Luschka into the CPA cistern. Alternatively a papilloma can arise from the small bit of choroid that has protruded through the foramen, and thus the lesion is totally within the cistern.

Vascular abnormalities can mimic ANs. Aneurysms cause a mass effect. They may be identified if there is an associated flow void or if clot within a partially thrombosed lumen is identified by typical MRI signal characteristics (Figs. 36 and 37). An artery may not have an actual aneurysm but can simply be tortuous or ectatic (dolichoectasia) and can cause symptoms by pressing on cranial nerves. The demonstration of a loop of the anterior inferior cerebellar artery close to a nerve or inside the canal is not uncommon but can be seen in a normal patient, and so the significance of this finding is not clear.

Lesions arising in the temporal bone such as a cholesterol cyst, cholesteatoma, or one of a variety of bone tumors are usually easily distinguished from AN. The origin outside the IAC is usually obvious. Occasionally a tumor, such as a paraganglioma, can have a substantial component protruding into the CPA cistern, but once again the finding of the characteristic erosion of the jugular fossa on CT or the characteristic black dots on MRI representing rapid flow in large tumor vessels (flow voids) indicate the true identity of the tumor (Fig. 38).

Finally a piece of polytef (Teflon) put in place to separate a vessel from a nerve can sometimes resemble a neuroma (Fig. 39). It can be dense on CT. There can be some enhancement of the contiguous tissues on CT or MRI. The site of the previous craniotomy is obvious, and the patient gives the appropriate clinical history.

Imaging in specific situations

Rule out acoustic neuroma

When the primary question is whether the patient has an AN, a gadolinium-enhanced MRI scan is the preferred imaging modality [3,18,45–47].

In the past one could not be completely sure that there was no AN unless the nerves could be visualized all the way through the IAC and no enlargement was present (Figs. 40 and 41). Now the contrast-enhanced MRI scan is considered sensitive enough that this is no longer necessary, and if no enhancement is seen, the examiner can confidently state that there is no AN present.

At our institution, we rely most strongly on high-resolution short TR/TE (T_1 weighted) axial images acquired after injection of gadolinium. Two interleaved sets of images are taken in one combined sequence, using 3-mm slices spaced every 4 mm. Because the slices are interleaved, the effective spacing is 2 mm. In other words, there is slight overlap and the entire canal is covered. Short TR/TE (T_2 weighted) sagittal and axial 5-mm slice thickness long TR/TE (T_2 weighted) sequences are also performed as part of the usual imaging protocol.

At many institutions, axial short TR/TE (T_1 weighted) images are performed before gadolinium is injected. Some radiologists perform T_1-weighted coronal sequences as well to have a second look at the canal. We do not find these necessary if the axial images are of excellent quality.

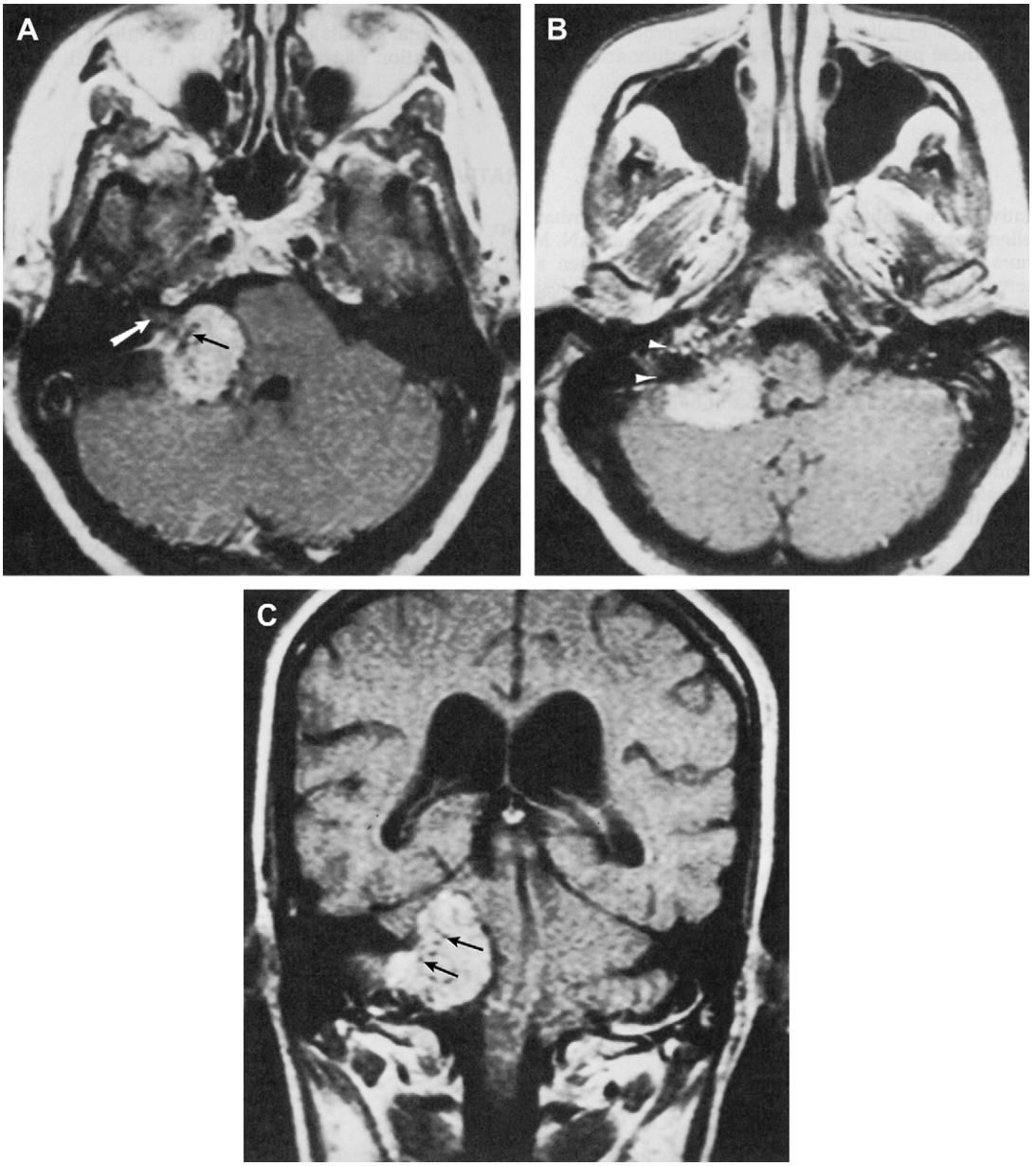

Fig. 38. (*A*) Paraganglioma protruding into CPA. Axial T_1-weighted postgadolinium image shows the lesion of the CPA cistern but it does not extend into the internal auditory canal (*white arrow*). There are small black dots that represent flow voids within the lesion (*black arrow*). (*B*) The lesion extends inferiorly and involves the bone along the lateral margin (*arrowheads*). (*C*) Coronal image shows the true origin of the lesion in the inferior temporal bone and the flow voids (*arrows*) characteristic of paraganglioma.

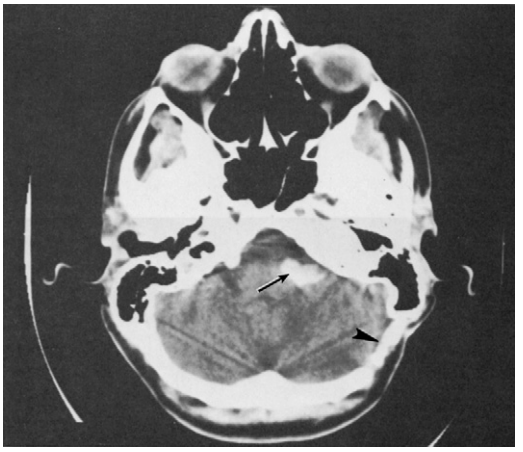

Fig. 39. Polytef (Teflon) in the CPA cistern. Increased radiodensity represents a piece of Teflon (*arrow*) used to separate nerve from vessel. Note the retromastoid craniotomy (*arrowhead*).

In some cases of acute symptoms, we have performed an axial T_1-weighted sequence before gadolinium injection to determine if there is abnormally high signal that is not due to enhancement. This is not likely to become part of our routine protocol. In cases in which there is higher than normal signal and there is a question of whether this represents enhancement or actually some other cause of increased signal (eg, hemorrhage), the scan can be repeated after several days when the gadolinium has disappeared from the system. If the signal is still present, it does not represent enhancement and some other explanation should be considered.

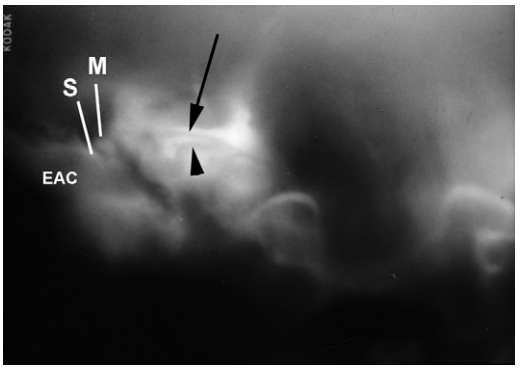

Fig. 40. Tomogram of the internal auditory canal after metrizimide instillation through a C1-2 puncture. The contrast can be followed into the canal outlining the facial nerve (*arrow*) and cochlear nerve (*arrowhead*). Normal size of the nerves indicates that there is no acoustic neuroma. EAC = external auditory canal; M = malleus; S = scutum.

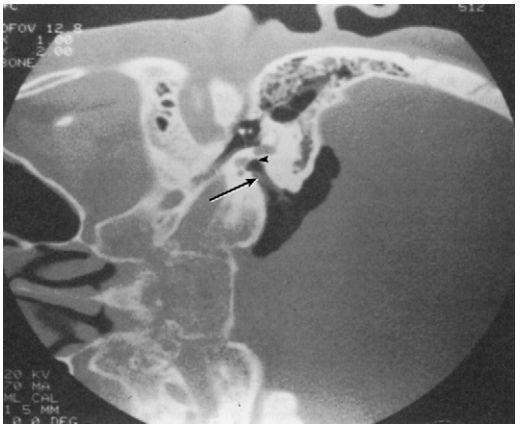

Fig. 41. Air cisternogram shows filling of the internal auditory canal (IAC) with air outlining the nerves (*arrow*). Note that the air passes all the way to the extreme lateral portion of the IAC (*arrowhead*).

Some patients cannot undergo MRI. There are contraindications such as pacemakers or certain aneurysm clips. Some patients are simply too claustrophobic to undergo the procedure. When a patient cannot undergo MRI, a contrast-enhanced, high-resolution CT scan is still a highly reliable examination. Almost all ANs will be found by high-quality modern CT scanning. Some clinicians prefer CT scanning, especially when the clinical picture is not as clear-cut and high-quality images of the otic labyrinth are desirable at the same time that the IAC is evaluated. Also CT remains more available in some locations and so becomes the initial study, with MRI reserved for the few cases in which the CT scan is considered equivocal.

Once an acoustic tumor is diagnosed by MRI, some surgeons request a CT scan for surgical planning if a posterior approach is contemplated in an attempt to preserve useful hearing (Fig. 42). A scan done for this purpose can be done without iodinated contrast material because the primary aim is not to see the tumor but to see the anatomy of the bone. On a high-resolution bone algorithm, the position of the vestibular aqueduct can be seen and the amount of bone separating the aqueduct from the lip of the IAC can be determined. The depth of the mastoid air cell system and the position of the sigmoid sinus are clearly shown, as is the relationship of the semicircular canals to the posterior wall of the petrous bone. Thus accidental violation of the labyrinth is, it is hoped, less likely.

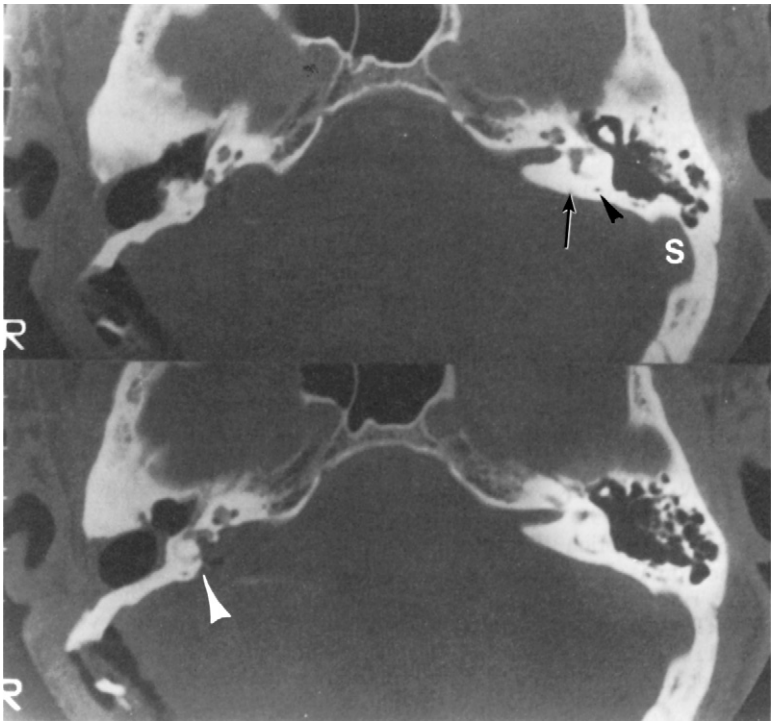

Fig. 42. Postsurgical resection acoustic neuroma right side. Bone algorithm shows the position of the vestibular aqueduct (*arrow*) on the right side. The surgical approach intersected the vestibular aqueduct on the left side (*white arrowhead*). This surgical defect extends into the vestibule. Other important structures include posterior semicircular canal (*black arrowhead*) and the sigmoid sinus close to the sinodural angle (S).

Postoperative evaluation

Once an AN has been removed, imaging may still play a role in following the patient to detect a recurrence. In hopes of retaining useful hearing, surgeons try meticulously to strip tumor away from the eighth cranial nerve. Then imaging is used to ensure that the tumor does not recur.

Either contrast-enhanced CT or contrast-enhanced MRI can be used. MRI is very sensitive. There is enhancement in the region of the resection in many cases, and this should not be considered to represent tumor (see Fig. 20). The dura can enhance and so can the reparative process in the region of the surgery. The initial examination can be considered as a baseline study. Future examinations are compared to find progressive changes that would indicate tumor regrowth. CT is again slightly less sensitive but, as with MRI, an enlarging area of enhancement on serial examinations suggests recurrence. Further experience is needed in the field of postoperative imaging before definitive statements regarding the significance of findings can be made.

Imaging is used to follow patients after gamma knife radiosurgery. The findings in these patients are covered in another article in this issue.

Summary

A negative high-quality, high-resolution, contrast-enhanced MRI scan is excellent evidence that a patient does not have an AN. Most nerve sheath tumors have a characteristic appearance, and when a tumor is detected there is seldom any doubt as to the identity of the lesion. There are other causes of enhancement, however, or of high signal that can be mistaken for an AN, and these must be kept in mind when a case is considered positive. In some cases, it may be appropriate to defer surgery to clarify a questionable finding by obtaining a follow-up scan.

CT is still a reliable examination. In addition to evaluating the IAC, valuable information about the architecture of the petrous bone and labyrinth is provided.

Improvements in imaging technology are occurring at a rapid rate. Thinner slices and more

rapid scan techniques will make MRI even more useful in evaluation of the IAC.

References

[1] Curati WL, Graif M, Kingsley DP, et al. MRI in acoustic neuroma: A review of 35 patients. Neuroradiology 1986;28:208–14.

[2] Gentry LR, et al. Cerebellopontine angle-perromastoid mass lesions. Comparative study of diagnosis with MR imaging and CT. Radiology 1987;162:513.

[3] House JW, Waluch V, Jackler RK. Magnetic resonance imaging in acoustic neuroma diagnosis. Ann Otol Rhinol Laryngol 1986;95:16–20.

[4] Jackler RK, Shapiro MS, Dillon WP, et al. Gadolinium-DTPA enhanced magnetic resonance imaging in acoustic neuroma diagnosis and management. Otolaryngol Head Neck Surg 1990; 102:670–7.

[5] Kingsley DPE, et al. Acoustic neuromas. Evaluation by magnetic resonance imaging. AJNR 1985;6:1.

[6] lindmann JA, Steinbrich W, Friedmann G, et al. Magnetic resonance tomography in acoustic neuromas. Laryngol Rhinol Otol (Stuttg) 1987;66:440–3.

[7] Lo WWM. Tumors of the temporal bone and the cerebellopontine angle. In: Som PM, Bergeron RT, editors. Head and Neck Imaging. 2nd edition. St. Louis: Mosby-Year Book; 1991. p. 1046–108.

[8] Mikhael MA, Wolff AP, Ciric IS. Current concepts in neuroradiological diagnosis of acoustic neuromas. Laryngoscope 1987;97:471–6.

[9] Press GA, Hesselink JR. MR imaging of cerebellopontine angle and internal auditory canal lesions at 1.5T. AJNR 1988;9:241.

[10] Stack JP, Ramsden RT, Antoun NM, et al. Magnetic resonance imaging of acoustic neuromas The role of gadolinium DTPA. Br J Radiol 1988;61: 800–5.

[11] Valvassori GE. Diagnosis of retrocochlear and central vestibular disease by magnetic resonance imaging. Ann Otol Rhinol Laryngol 1988;97:19–22.

[12] Valvassori GE, Garcia Morales F, Palacios E, et al. MR of the normal and abnormal internal auditory canal. AJNR 1988;9:115–9.

[13] Wilms G, Decrop E, Plets C, et al. Magnetic resonance imaging in acoustic neuroma. Comparison with CT. J Beige Radiol 1989;72:151–8.

[14] Glasscock ME III, Levine SC, McKennan KX. The changing characteristics of acoustic neuroma patients over the last 10 years. Laryngoscope 1987; 97:1164–7.

[15] Bassi P, Piazza P, Cusmano F, et al. MR cisternography of the cerebellopontine angle and internal auditory canal in diagnosis of intracanalicular acoustic neuroma. Neuroradiology 1990;31:486–91.

[16] Fuse T, Nagai H, Ohara S, et al. Massive hemorrhage within an acoustic neuroma. Case report. Neurol Med Chir (Tokyo) 1989;29:933–7.

[17] Felix R, Schorner W, Laniado M, et al. Contrast media in magnetic resonance tomography. A review. 2. Biological basis, research technic and clinical application of gadolinium-DTPA in the diagnosis of intracranial tumors. ROFO 1985;143:9–14.

[18] Sidman JD, Carrasco VN, Whaley RA, et al. Gadolinium. The new gold standard for diagnosing cerebellopontine angle tumors. Arch Otolaryngol Head Neck Surg 1989;115:1244–7.

[19] Valvassori GE, Mafee MF, Dobben GD. Computerized tomography of the temporal bone. Laryngoscope 1982;92:562.

[20] Moller A, Hatam A, Olivecrona H. Diagnosis of acoustic neuroma with computed tomography. Neuroradiology 1978;17:25.

[21] Valavanis A, Schubiger O, Naidich TP. Clinical Imaging of the Cerebellopontine Angle. Berlin. Springer-Verlag; 1986.

[22] Suzuki M, Takashima T, Kadoya M, et al. MR of acoustic neuromas— relationship to cranial nerves. Radiat Med 1989;7:169–72.

[23] Bognanno JR, Edwards MK, Lee TA, et al. Cranial MR imaging in neurofibromatosis. AJR 1988;151: 381–8.

[24] Cammarata CA, Deveikis JP, Schellinger D, et al. Neuroradiology case of the day. Neurofibromatosis 2. AJR 1990;154:1337–8.

[25] Costantino PD, Friedman CD, Pelzer HJ. Neurofibromatosis type II of the head and neck. Arch Otolaryngol Head Neck Surg 1989;115:380–3.

[26] Kitamura K, Senba T, Komatsuzaki A. Bilateral internal auditory canal enlargement without acoustic nerve tumor in von Recklinghausen neurofibromatosis. Neurofibromatosis 1989;2:47–52.

[27] Mulvihill JJ, Parry DM, Sherman JL, et al. NIH conference. Neurofibromatosis 1 (Recklinghausen disease) and neurofibromatosis 2 (bilateral acoustic neurofibromatosis). An update. Ann Intern Med 1990;113:39–52.

[28] New PF, Bachow TB, Wismer GL, et al. MR imaging of the acoustic nerves and small acoustic neuromas at 0.6 T. Prospective study. AJR 1985;144: 1021–6.

[29] Haberman RS II, Kramer MB. False-positive MRI and CT findings of an acoustic neuroma. Am J Otol 1989;10:301–3.

[30] Millen SJ, Daniels DL, Meyer GA. Gadolinium-enhanced magnetic resonance imaging in temporal bone lesions. Laryngoscope 1989;99:257–60.

[31] Tien R, Dillon WP, Jackler RK. Contrast-enhanced MR imaging of the facial nerve in 11 patients with Bell's palsy. AJR 1990;155:573–9.

[32] Anderson RE, Laskoff JM. Ramsay Hunt syndrome mimicking intracanicular acoustic neuroma on contrast-enhanced MR. AJNR 1990;11:409.

[33] Seltzer S, Mark AS. Contrast enhancement of the labyrinth on MR scans in patients with sudden hearing loss and vertigo: Evidence of labyrinthine disease. AJNR 1991;12:13.

[34] Weissman JL, Curtin HD. Abnormal signal of the otic labyrinth on MRI. AJNR; 1992, in press.
[35] Mark AS, Seltzer S, Harnsberger R. Gadolinium MR imaging in patients with hearing loss. More than "rule out" acoustic neuroma. Exhibited at the 76th Scientific Assembly and Annual Meeting of the Radiological Society of North America, November 25–30, 1990, Chicago.
[36] Bilaniuk LT. Adult infratermporal tumors. Semin Roentgenol 1990;25:155–73.
[37] Mikhael MA, Ciric IS, Wolff AP. Differentiation of cerebellopontine angle neuromas and meningiomas with MR imaging. J Comput Assist Tomogr 1985; 9:852–6.
[37a] Daniels DL, Millen SJ, Meyer GA, et al. MR detection of tumor in the internal auditory canal. AJR 1987;148:1219–22.
[38] Valavanis A, et al. CT of meningiomas on the posterior surface of the petrous bone. Neuroradiology 1981;22:111.
[39] Langman AW, Jackler RK, Althaus SR. Meningioma of the internal auditory canal. Am J Otol 1990;11:201–4.
[40] Lo WWM, et al. Intratemporal vascular tumors. Evaluation with CT. Radiology 1986;159:181.
[41] Lo WWM, et al. Intratemporal vascular tumors. Detection with CT and MR. Radiology 1989;171:443.
[42] Braun IF, et al. Dense intracranial epidermoid tumors. Radiology 1977;122:717.
[43] Suss RA, Maravilla KR, Thompson J. MR imaging of intracranial cysticercosis. Comparison with CT and anatomopathologic features. AJNR 1986; 7:235.
[44] Zee CS, et al. MR imaging of neurocysticercosis. J Comput Assist Tomogr 1988;12:927.
[45] Curati WL, Graif M, Kingsley DP, et al. Acoustic neuromas: Gd-DTPA enhancement in MR imaging. Radiology 1986;158:447–51.
[46] Haughton VM, et al. Sensitivity of Gd-DTPA-enhanced MR imaging of benign extraaxial tumors. Radiology 1988;166:829–33.
[47] Vogl T, Bauer M, Hahn D, et al. Magnetic resonance tomography in suspected acoustic neurinoma. Technic and differential diagnosis. ROFO(2) 1986;145:631–8.
[48] Daniels DL, Schenck JF, Foster T, et al. Surface-coil magnetic resonance imaging of the internal auditory canal. AJR 1985;145:469–72.
[49] Morrison AW, King TT. Space-occupying lesions of the internal auditory meatus and cerebellopontine angle. Adv Otorhinolaryngol 1984;34:121–42.